Supplementary Information

Genetic and functional analyses demonstrate a role for abnormal glycinergic signaling in autism

Marion Pilorge, Coralie Fassier, Hervé Le Corronc, Anaïs Potey, Jing Bai, Stéphanie De Gois, Elsa Delaby, Brigitte Assouline, Vincent Guinchat, Françoise Devillard, Richard Delorme, Gudrun Nygren, Maria Råstam, Jochen C. Meier, Satoru Otani, Hélène Cheval, Victoria M. James, Maya Topf, T. Neil Dear, Christopher Gillberg, Marion Leboyer, Bruno Giros, Sophie Gautron, Jamilé Hazan, Robert J. Harvey, Pascal Legendre, Catalina Betancur

SUPPLEMENTARY METHODS

Mutation screening

Genomic DNA was extracted from blood leukocytes or B lymphoblastoid cell lines using standard procedures. The nine *GLRA2* coding exons and intron-exon boundaries were PCR amplified using specific primers designed with Primer3 v.0.4.0 (http://frodo.wi.mit.edu; Supplementary Table S7). Alternative splicing of exon 3 generates two splice variants, GlyR α2A and GlyR α2B, differing by only two amino acids at positions 85 and 86; specific primers were designed to span the two alternative exons 3 for sequence analysis. The PCR reaction was performed with *Taq* DNA polymerase (Invitrogen, Carlsbad, CA) in 20 µl reaction mix (20 ng genomic DNA, 0.5 µM of each primer, 1.5 mM $MgCl_2$, 0.2 mM dNTP, and 1X Taq Polymerase PCR Buffer). Two PCR protocols were used: (1) standard protocol (exons 5, 7, and 8): 95°C for 30 sec, followed by 35 cycles at 95°C for 30 sec, 58°C (exon 7) or 60°C (exons 5 and 8) for 30 sec, 72°C for 30 sec, with a final cycle at 72°C for 10 min; and (2) touchdown protocol (exons 1, 2, 3, 4, 6, and 9): 95°C for 10 min followed by 20 cycles at 95°C for 30 sec, 65-55°C (exon 1), 62-56°C (exons 2, 3, 6, and 9) or 56-50°C (exon 4) for 30 sec; 72°C for 1 min, followed by 20 cycles at 95°C for 30 sec; 55°C (exon 1), 56°C (exons 2, 3, 6, and 9) or 50°C (exon 4) for 30 sec; 72°C for 1 min, with a final cycle at 72°C for 10 min. PCR products were visualized in a 1% agarose gel and purified using exonuclease I (USB Corporation, Cleveland, OH) and shrimp alkaline phosphatase (USB). Sequence analysis was performed by direct sequencing of the PCR products using BigDye Terminator v3.1 mix (Applied Biosystems, Foster City, CA) followed by capillary electrophoresis on an ABI 3730 sequencer (Applied Biosystems).

Real-time quantitative PCR and long-range PCR

Quantitative PCR (qPCR) was performed on a LightCycler 480 real-time PCR system (Roche, Indianapolis, IN) using the Universal Probe Library (UPL) system from Roche, to confirm and map the deletion in Patient 1. Long-range PCR was carried out using the Expand Long Template PCR System from Roche, followed by sequencing of the junction fragment.

RNA extraction and reverse transcription PCR

Five ml of whole blood from Patient 1, his mother and healthy controls were collected directly into PAXgene blood RNA tubes (PreAnalytiX, Hombrechtikon, Switzerland). Total RNA was isolated using the PAXgene blood RNA kit according to the protocol supplied by the manufacturer. RNA quality was determined by running samples on a 1% agarose gel. Total RNA was subjected to reverse transcription using Superscript II reverse transcriptase (Invitrogen) and random primers. PCR experiments were performed using 50-100 ng cDNA as template.

Determination of X-inactivation pattern

X chromosome inactivation was determined by evaluating the methylation status of the polymorphic $(CAG)_n$ repeat located in the first exon of the androgen receptor gene *AR*, as previously described.[1] X chromosome inactivation was considered skewed if the ratio was ≥80:20.

Immunohistochemistry

Chinese hamster ovary (CHO) cells were immunolabeled using goat polyclonal antiserum against the human GlyR α2 subunit (1:300; GlyR α2 N-18: SC-17279; Santa Cruz Biotechnology, Santa Cruz, CA). Cells were fixed in 2% paraformaldehyde, washed in PBS, and incubated in PBS-NH_4Cl (100 mM) for 20 min, followed by blocking in 20 mM PBS with 0.25% fish gelatin for 30 min at room temperature. Cells were subsequently incubated with

the first antibody at room temperature for 2 h and then with a donkey anti-goat Alexa Fluor 594 (red) secondary antibody (1:1000; A11058, Life Technologies, Carlsbad, CA) at room temperature for 2 h. Both antibodies were diluted in the blocking solution. In some experiments, cells were permeabilized with Triton X-100 (0.2% Triton X-100 in PBS-gelatin solution) for 30 min at room temperature, to visualize the deleted construct retained in the cytoplasm. Images were taken using a Leica SP5 confocal microscope (Leica Microsystems, Wetzlar, Germany).

Cell surface biotinylation and western blotting

Biotinylation of transfected CHO cells was performed using the Pierce Cell Surface Protein Isolation Kit (Thermo Scientific, Rockford, IL) according to the manufacturer's protocol. Briefly, CHO cells were washed with PBS and incubated for 30 min at 4°C in sulfo–NHS–SS–biotin in PBS. After terminating the reaction using the quenching solution, cells were harvested and washed three times with Tris-buffered saline to remove unbound biotin. Cells were lysed for 30 min at 4°C with sonication every 5 min to improve solubilization and then centrifuged at 10 000 g for 2 min. Supernatants were incubated in NeutrAvidin beads for 1 h at room temperature with rotation to isolate the biotinylated surface proteins. After washing and centrifugation to remove unbound proteins, bound biotinylated proteins were eluted in SDS–PAGE buffer containing 50 mM DTT for 1 h at room temperature.

The protein concentration was quantified using the Bradford method (Bio-Rad, Hercules, CA). For western blotting, protein extracts were separated by size on 10% Bis-Tris/MES SDS-polyacrylamide gels (Life Technologies) and transferred to nitrocellulose membranes (Life Technologies). Membranes were incubated in blocking buffer for 30 min at room temperature, washed three times in PBS-Tween 0.1% and incubated overnight at 4°C with primary antibodies: goat anti-GlyR α2 (1:200, GlyR α2 N-18: SC-17279, Santa Cruz Biotechnology), rabbit anti-EGFP (1:1000, A11122, Life Technologies), and mouse anti-GAPDH (1:5000, CB1001, Calbiochem, Darmstadt, Germany). GAPDH (endogenously expressed) and EGFP (co-transfected) were used to confirm that intracellular proteins were not labeled with biotin. Bound GlyR α2 antibodies were detected using rabbit anti-goat antibody (1:5000, 305-005-003, Jackson Immunoresearch, West Grove, PA), followed by horseradish-peroxidase-conjugated anti-rabbit IgG (1:10000, 111-035-006, Jackson Immunoresearch). EGFP and GAPDH primary antibodies were detected using horseradish-peroxidase-conjugated anti-rabbit (1:10000, 111-035-006, Jackson Immunoresearch) or anti-mouse IgG (1:10000, A3682, Sigma), respectively. Chemiluminescence was revealed using the SuperSignal West Pico kit (ThermoScientific). Immunoblots were scanned using a LAS-3000 imaging system (Fujifilm, Düsseldorf, Germany) and quantified using MCID software (Imaging Research, St. Catharines, ON, Canada). Data were normalized for transfection efficiency by measuring fluorescence of co-transfected EGFP with flow cytometry.

Zebrafish knockdown and rescue experiments

Zebrafish embryos were raised at 28°C in E3 medium supplemented with 0.2 mM 1-phenyl-2-thiourea (PTU, Sigma) to prevent pigment formation and staged according to Kimmel *et al.*[2] A morpholino oligonucleotide (*glra2* MO: 5'-TTTGACCGAAGGGCGAGTCATTCCT-3'), predicted to specifically block *glra2* translation initiation site without affecting the translation of other zebrafish GlyR α subunits (*glra1*, *glra3*, *glra4a,* and *glra4b*), was designed by GeneTools (Philomath, OR) and injected at 1 pmole per embryo. For rescue experiments, the wild-type, mutated, and deleted versions of human *GLRA2* cDNA were subcloned into the pCS2+ expression vector and *in vitro* transcribed using SP6 mMessage mMachine kit (Ambion Europe, Huntingdon, UK). The resulting mRNAs were injected at 100 pg in one-cell stage wild-type embryos while *glra2* MO was subsequently injected at the two-cell stage. Doubly injected, morphant and control embryos were fixed at 28 h post fertilization in 4% paraformaldehyde for 2 h at room temperature. Whole-mount immunohistochemistry using the primary antibody znp-1 (ZIRC, University of Oregon, OR) at 1:100 was carried out according to standard procedures as previously reported.[3] Images were acquired using a fluorescence microscope equipped with an Apotome module (Axiovert 200M, Carl Zeiss France, Le Pecq, France) and processed with the NIH ImageJ software. Each experiment was reproduced three or four times and statistical analyses were performed using the Student's unpaired *t*-test.

***In situ* hybridization in zebrafish**

Digoxigenin-labeled antisense and sense RNA probes were synthesized from a linearized TOPO TA cloning pcr4 vector containing a *glra2* cDNA fragment (amplified with the primers glra2-F 5'-TCTGTACAGCATCAGGCTGACG-

3' and glra2-R 5'-CTGATGATCTTATACGTGATCC-3') using T3 and T7 RNA polymerases (Roche) according to the supplier's instructions. Whole-mount *in situ* hybridization experiments were carried out at 24 h post-fertilization (hpf) using standard procedures.[4] Pictures were acquired with a binocular stereomicroscope (Leica M165C) combined with a camera (Leica IC80 HD).

Fluorescence-activated cell (FAC) sorting of zebrafish spinal motor neurons and RT-PCR analysis

FAC sorting of zebrafish spinal motor neurons was performed using the transgenic line Tg(*mnx1*:EGFP), which specifically expresses enhanced green fluorescent protein (EGFP) in spinal motor neurons.[5] The trunks of 160 Tg(*mnx1*:EGFP) transgenic embryos were dissected at 24 hpf and collected in Marc's Modified Ringer (MMR: 100 mM NaCl, 2 mM KCl, 1 mM $MgSO_4$, 2 mM $CaCl_2$, 5 mM Na-Hepes, and 0.1 mM EDTA, pH 7.8). Trunks were next chemically dissociated in custom ATV solution (0.6 mM EDTA, 5.5 mM glucose, 5.4 mM KCl, 136.8 mM NaCl, and 5.5 mM Na_2CO_3; Irvine Scientific, Santa Ana, CA) supplemented with 0.25% of trypsin for 20 min at 27°C, and mechanically dissociated in 1 ml of L-15 medium (Invitrogen) supplemented with 1% of fetal bovine serum (FBS) using a drawn-out Pasteur pipette. Cells were centrifuged at 300 g for 5 min, resuspended in 1 mL of L-15 medium + 1% FBS, and filtered through a 30 µm nylon mesh (BD Falcon, BD Biosciences, San Jose, CA) to remove undissociated tissue before proceeding with FAC sorting. EGFP-positive and -negative cells were sorted using a MoFlo Astrios flow cytometer (Beckman Coulter, Fullerton, CA). The sorting was performed at room temperature with a laser set at 488 nm and 150 mW (OPSL, Coherent, Santa Clara, CA). Cells were carefully selected according to their size, complexity and fluorescence intensity. To minimize RNA degradation, sorted cells were directly collected in RNAprotect Cell Reagent (Qiagen, Valencia, CA). Sorted cells were pelleted at 300 g for 5 min and total RNAs were isolated from EGFP+ and EGFP– cells using the RNeasy Micro Kit (Qiagen) according to the manufacturer's instructions. RNA concentration and purity were determined using a NanoDrop spectrophotometer (Thermo Scientific, Wilmington, DE). RT-PCR analysis was performed from equal amounts of EGFP+ and EGFP– mRNA (0.5 to 10 ng) using the SuperScript III One-Step RT-PCR System with Platinum *Taq* DNA Polymerase (Invitrogen) and the primers shown in Supplementary Table S9. RT-PCR amplification of transcripts specifically expressed in interneurons (*tbx16*), Rohon-Beard sensory neurons (*kitb*) and muscle cells (*myhz1.1*), or enriched in spinal motor neurons (*chodl* and *mnx2a*), was used to confirm the purity of the EGFP+ cell population.

Generation of *Glra2* knockout mice

Glra2 mutant mice were generated by targeted deletion of exon 7 encoding transmembrane domains 1 and 2 (TM1-TM2). The targeting vector was constructed in pEasyFlox to contain loxP sites flanking exon 7 of *Glra2* and a neomycin cassette. The targeted construct was introduced into the 129/SvJae derived PC3 ES cell line for homologous recombination. Correctly targeted ES cells were selected and injected into C57BL/6J blastocysts to obtain *Glra2* chimeric mice. Because the PC3 ES cell line contains a transgene driving expression of cre recombinase under the control of the protamine 1 promoter,[6] cre-mediated excision of exon 7 and/or the neomycin cassette was induced in the male chimeras germ line during the terminal haploid stages of spermatogenesis. Mice containing the *Glra2* exon 7 deleted allele were obtained by mating chimeric mice with wild-type mice. Targeted disruption of *Glra2* in the progeny was confirmed by PCR and Southern blotting. Mice were genotyped by PCR analysis using two sets of primers (F1: 5'-CACATGAACCCCAACACAAG-3' and R1: 5'-AATGTTGCAAACACCAACGA-3'; F2: 5'-TGATCCTTTTCTGCTTCCAG-3' and R2: 5'-GCTTTCGACAAGACCTTTGG-3'). Mutant mice were backcrossed to C57BL/6J for at least eight generations before experiments.

No compensatory increases in *Glra1*, *Glra3*, or *Glrb* expression were observed in the prefrontal cortex of *Glra2* mutant mice compared to control littermates (Supplementary Figure S10).

Behavioral assays

Behavioral experiments were conducted in dedicated behavioral testing rooms during the standard light phase, usually between 9 AM and 6 PM. One week prior to testing, mice were handled daily for 5 min. Mice were moved from the animal facility to the testing room for at least 1 h prior to behavioral testing. Six independent cohorts of wild-type (WT) and hemizygous ($Glra2^{-/Y}$) male mice were tested. The first cohort included 16 WT and 15 $Glra2^{-/Y}$ littermates, except when noted (Supplementary Table S6). The order of the tests was as follows: spontaneous locomotion, elevated plus maze, light-dark box, open-field test, sociability and preference for social novelty, marble burying, self-grooming/stereotypies, olfactory habituation/dishabituation test, novel object recognition task, novel location recognition task, inverted wire hang, Morris water maze, accelerating rotarod, and hole board. A second (12 mice per genotype) and a third cohort (8 mice per genotype) were

tested for nesting and social interaction with juveniles. Three additional independent replication cohorts (*n* = 9 WT, 6 *Glra2*$^{-/Y}$; *n* = 7 WT, 8 *Glra2*$^{-/Y}$; *n* = 11 WT, 11 *Glra2*$^{-/Y}$) were examined in the novel object recognition task and the sociability and preference for social novelty test.

***Spontaneous locomotion*.** Horizontal (locomotion) and vertical (rearing) activities were measured individually in Plexiglas cages (20 x 15 x 25 cm) with automatic monitoring of photocell beam breaks every 5 min for 2 h (Imetronic, Pessac, France). Mice were tested at 7 weeks of age (not shown) and again at 19 weeks of age (Supplementary Figure S6). No difference between genotypes was observed at either age.

***Open-field test*.** The test took place in a white open-field apparatus (110 x 110 x 35 cm) under dim light (~30 lux). Animals were individually placed in the corner of the open-field and were allowed to explore for 10 min. A video tracking system, which included a computer-linked overhead video camera, was used to monitor locomotor activity. Distance travelled was measured every 2 min and total distance over the 10-min session was scored using an image analyzer (ViewPoint, Lyon, France).

***Accelerating rotarod*.** Mice were placed on a rotating rod (model LE8200, Bioseb, Chaville, France) that accelerated from 0 to 40 revolutions per minute over a 5-min period. Five trials were performed for each subject, with an inter-trial time of 30 min. The maximum duration of each trial was 5 min. The time to fall off the rod was recorded.

***Inverted wire hang task*.** The task was performed by placing the mouse on the wire bars of a standard mouse cage lid, allowing the mouse to obtain its grip and then swiftly inverting the lid over a cage covered with foam to avoid injury. Latency to fall into the cage was measured over a 60 s maximum test session. Mice that fell in less than 10 s were given a second trial. A clean wire lid was used for each mouse.

***Light-dark box*.** The apparatus consists of a polypropylene chamber (47 x 21.5 x 21.5 cm) unequally divided into two chambers by a partition containing a small opening. The large chamber is brightly illuminated (400 lux), while the small chamber is dark (<10 lux). Mice were placed into the dark side and allowed to move freely between the two chambers for 10 min. Latency to enter the light side, duration, and number of entries to light and dark compartments were determined by an observer. An entry was defined as the mouse placing all four paws into the zone. The apparatus was cleaned with 70% ethanol and water after each subject.

***Elevated plus maze*.** The maze had a central platform, two closed arms with walls 17 cm in height, and two open arms; the arms were 30 cm long and 7 cm large and the maze was elevated 50.5 cm from the floor. Mice were placed on the center section and allowed to freely explore the maze for 5 min under a light intensity of ~30 lux. Entries and time in each arm were recorded by an overhead video camera linked to a computer. An open or closed arm entry was defined as the mouse placing all four paws into an arm. The maze was cleaned with 70% ethanol and water between each animal.

***Hole board*.** The test was performed as previously described[7] with modifications. The apparatus was made of blue Plexiglas (42 x 42 x 3 cm) with 16 equally spaced holes (2 cm in diameter) arranged in four rows (homemade). Mice were allowed to explore the hole board for 10 min. The behavior was recorded by a computer-linked overhead video camera. The number of head-dips and the number of holes multiply visited over the 10-min session were scored by a trained observer.

***Marble burying*.** Mice were individually assessed in a clean cage (36.5 x 20.5 x 14 cm) filled with 6 cm bedding material, overlaid with 12 black glass marbles (15 mm in diameter) equidistant in a 4 x 3 arrangement. Testing consisted of a 20 min exploration period, during which the number of marbles buried (>50% marble covered) was scored.

***Grooming and stereotypies*.** Mice were individually assessed in a clean cage (36.5 x 20.5 x 14 cm) with bedding material, under a light intensity of ~30 lux. After 10 min of habituation, animals were video recorded for 10 min and later observed for self-grooming behavior defined as paw licking, head wash, and body groom, and other spontaneous motor stereotypies such as jumping and bar-biting. No difference between genotypes was observed (data not shown).

***Sociability and preference for social novelty*.** Sociability and preference for social novelty were assayed as previously described,[8] except that the tests were conducted in a square open-field (42 x 42 x 25 cm) with two

transparent plastic boxes (13 x 11 x 6.5 cm) with a total of 28 holes (10 mm diameter) in them, allowing visual, olfactory, auditory, and partial tactile contact. During habituation, the test mouse was placed in the empty open-field and allowed to explore for 5 min. Immediately after the habituation period, the subject was briefly confined in a corner of the open-field while the two boxes were placed on opposite corners of the apparatus, with an unfamiliar adult C57BL/6J male (stranger 1) that had no prior contact with the subject mouse in one of the two boxes. The location of the stranger mouse was systematically alternated. The test mouse was then released and allowed to explore during 10 min. Immediately afterwards, mice were tested in a second 10 min session to quantify social preference for a new stranger. A second, unfamiliar adult C57BL/6J male (stranger 2) was placed in the box that had been empty in the first 10 min session. The subject mouse had a choice between the first, already-investigated mouse (stranger 1), and the novel unfamiliar mouse (stranger 2). The behavior was recorded during the entire test by a computer-linked overhead video camera and an experimenter scored the time spent exploring both boxes in each session. The apparatus was cleaned with 70% ethanol and water between subjects.

***Olfactory habituation/dishabituation test*.** The test was conducted as previously described.[9] Non-social and social odors were presented on a series of cotton swabs inserted into a clean cage sequentially, in the following order: water, water, water (distilled water); almond, almond, almond (1:100 dilution artificial almond flavoring); vanilla, vanilla, vanilla (1:100 dilution artificial vanilla flavoring); social 1, social 1, social 1 (swiped from the bottom of a cage housing unfamiliar male C57BL/6J mice); and social 2, social 2, social 2 (swiped from the bottom of a second cage housing unfamiliar male 129/SvJ mice). Each test session was conducted in a clean cage containing fresh litter. Each swab was presented for a 2 min period, immediately following the last swab presentation. Time spent sniffing the swab was recorded by an investigator. Sniffing was scored when the nose was within 2 cm of the cotton swab.

***Social interaction with juveniles*.** Adult mice were individually tested in clean cages with fresh litter and paired with an unfamiliar C57BL/6J male juvenile (3-4 weeks old). The test session lasted 10 min. Social behavior was monitored with a computer-linked overhead video camera and videos were subsequently scored by a trained investigator using Labwatcher (Viewpoint) on measures of nose-to-nose and nose-to-anogenital sniffing.

***Nest formation*.** The test was conducted as previously described.[10] Nesting material (pressed cotton) was placed in the home cage of grouped mice for two days before the experiment to avoid neophobia. On the day of the test, approximately 1 h before the dark phase, mice were transferred to individual testing cages with fresh litter and 2-3 g of pressed cotton in each cage, with food and water available *ad lib*. The nests were assessed the next morning on a rating scale of 1-5, as follows: (1) nesting material not noticeably touched, (2) nesting material partially torn, (3) nesting material mostly shredded but often no identifiable nest site, (4) an identifiable but flat nest, and (5) a (near) perfect nest.

Novel object and novel location recognition tasks. The tasks were performed in a round open-field (40 cm in diameter) containing litter that had been exposed to other mice before testing to provide a constant odor level in the open-field under a light intensity of ~30 lux. Stimuli consisted of colored animal figurines (4 x 4 x 5 cm) made of resin.

Habituation. Before the experimental sessions, animals were habituated during four days to the apparatus to reduce stress due to the novel environment. On day 1, mice were introduced in the open-field together with their cage mates for 30 min. On days 2, 3, and 4, mice experienced the open-field individually for two 10 min trials with an inter-trial time of 5 h. On day 4, a couple of identical objects that were not used later during the test were placed in the open-field in order to reduce stress due to the appearance of novel objects in the arena.

Novel object recognition task. The test consisted of a familiarization phase followed by a recognition test with a memory delay interval of either 10 min (short-term memory test) or 24 h (long-term memory test). During the familiarization phase, each mouse received three consecutive 5-min exposures to the open-field containing a pair of identical objects, with an inter-trial time of 5 min. The mouse was placed in a temporary holding cage between trials and objects were cleaned after each trial. The recognition test was run either 10 min or 24 h after the familiarization phase ended. One clean familiar object and one clean novel object were placed in the arena, where the two identical objects had been located during the familiarization phase, and the mouse was returned to the open-field for a 5-min recognition test. The familiarization phase and the recognition test were videotaped and subsequently scored by a trained investigator. Object exploration was

defined as any investigative behavior (sniffing or deliberate contact) within 2 cm of the objects. Memory was operationally defined by the discrimination index (DI) for the novel object, calculated as the time spent exploring the novel object divided by the total time spent exploring both objects [Discrimination Index = (novel object exploration time/total exploration time)×100]. The time spent sniffing two identical objects during the familiarization phase confirmed the lack of a side bias.

Novel location recognition task. This task assesses the ability of mice to recognize a novel spatial arrangement of familiar objects. Procedures were as described in the novel object recognition task, except that identical copies of objects were used in the recognition phase, with one of them moved to a new location in the open-field. Mice were allowed to explore two familiar objects, with one in a new location.

***Morris water maze*.** Procedures were performed as previously described,[11,12] with minor modifications.

Apparatus. The water maze consists of a circular stainless steel pool (150 cm in diameter, 30 cm in height) filled to a depth of 16 cm with water maintained at 20–22°C and made opaque using a white aqueous emulsion (Acusol OP 301 opacifier, Rohm Ihaas, Paris, France). The escape platform was made of rough stainless steel and measured 9 cm in diameter. A video tracking system, which included a computer-linked overhead video camera and an image analyzer (ViewPoint), was used to monitor activity.

Non-spatial learning (cued version). Initial training consisted of cued navigation to a visible platform during four consecutive days with four trials per day and an inter-trial time of 10 min. The extra-maze cues were hidden with a curtain placed around the water maze during the trials, and the platform location was varied randomly from trial to trial. Mice were placed in one of four starting locations facing the pool wall and allowed to swim until they found the platform. The time taken to reach the platform (latency) was recorded. If the mouse located the platform within 90 s, the mouse was allowed to remain on it for 30 s before being removed to the home cage. Mice that failed to find the platform within 90 s were manually guided to the platform and allowed to remain on it for 30 s.

Spatial learning. In the hidden-platform task, the platform was submerged 1 cm below the surface of the water and mice had to navigate using extra-maze cues that were placed on the walls of the testing room to find the platform. The location of the platform was fixed over a series of four trials per day during five consecutive days, with an inter-trial time of 10 min. Mice were placed into the pool at one of the four starting locations and allowed to swim until they found the platform, or for a maximum of 90 s. Mice that failed to find the platform within 90 s were guided to it. The animal then remained on the platform for 30 s before being removed from the pool. The time taken to reach the platform was recorded. Two probe trials were conducted, 10 min and 24 h after the last trial on day 5, to assess short-term and long-term memory. In the probe tests, the platform was removed and mice were allowed to swim for 60 s. Latency to reach the supposed platform location, percent time spent in the quadrant, and platform crossing were recorded.

Spatial reversal learning. To investigate the flexibility of cognitive processes in *Glra2*$^{-/Y}$ mice, the spatial reversal water maze test was performed. After the last probe trial in the spatial learning test, the escape platform was moved from the original position to the opposite quadrant. Four trials per day were performed during two consecutive days followed by two probe tests without the platform, 10 min and 24 h after the last trial.

Real-time reverse transcription PCR in mouse brain

RNA samples from prefrontal cortex were obtained from embryonic (E12 and E14), neonatal (P0 and P5), juvenile (P15 and P20), and adult WT mice to determine *Glra2* transcript levels (Supplementary Figure S9). RNA was also isolated from the prefrontal cortex of *Glra2*$^{-/Y}$ mice at E14, P0, and P15 to determine transcript levels of *Glra1*, *Glra3*, *Glra4*, and *Glrb,* in order to explore potential compensatory mechanisms in mutant mice compared to WT (Supplementary Figure S10). Total RNA was extracted using RNeasy kit (Qiagen), treated with DNase I (Invitrogen), and used to produce total cDNA with Superscript II reverse transcriptase (Invitrogen) and random primers. Total cDNA (25 ng) was used for the qPCR, performed as described above using the UPL system from Roche. Intron-spanning primers were designed using the ProbeFinder v2.04 software (Supplementary Table S8). The gene encoding mouse β-glucuronidase (*Gusb*) was used as control. The relative mRNA expression levels were calculated with a comparative threshold cycle (Ct) method using *Gusb* as control [ΔCt=Ct(target gene)-Ct(*Gusb*)], and a control sample [ΔΔCt=ΔCt(sample test)-ΔCt(control sample)]. The relative transcript number was then calculated as $2^{-\Delta\Delta Ct}$.

SUPPLEMENTARY CLINICAL DESCRIPTION

Patient 1: *142 kb deletion of GLRA2, maternal*

Patient 1 is the only child of healthy non-consanguineous parents of European origin. The family history was negative for psychiatric or cognitive disorders, except for alcohol dependence in the maternal grandfather. He was born at 38 weeks of gestation after an uneventful pregnancy and delivery. Birth weight was 3,200 g. He walked at 12 months; speech development was delayed, with first words at 24 months and first phrases at 60 months. Manifestations of autism were initially noted at the age of 2 years. He had recurrent otitis media, requiring placement of pressure equalization tubes at 36 months. He has bilateral high-grade myopia, as his mother and maternal grandfather, and wears glasses. There was no history of epilepsy.

When evaluated at 10 years 9 months, he had functional language and met criteria for autism according to the ADI-R (social: 21, verbal communication: 16, repetitive behaviors: 7, abnormality before age 36 months: 2). Cognitive evaluation with the Wechsler Intelligence Scale for Children-Third Edition (WISC-III) showed a verbal IQ of 93, a performance IQ of 75, and a full-scale IQ of 82. The Kaufman Assessment Battery for Children results were: sequential processing scale 122, simultaneous processing scale 114, mental processing composite 120, and nonverbal scale 113.

On physical examination at the age of 11 years 4 months, his weight was 28 kg (-1.3 SD), height 144 cm (+0.3 SD), and head circumference 55 cm (+0.7 SD). The physical exam was normal, with no dysmorphic features; his neurological exam was normal except for difficulties with motor coordination and clumsy gestures.

As a young adult, he lives with his parents and works in a sheltered environment; he uses public transportation independently to go to work. He has no friends and spends most of his free time at the computer, playing video games. Although he can talk about things that interest him, he is unable to have a normal conversation. He exhibits ritualistic tendencies and marked resistance to change.

Clinical work-up included normal karyotype, negative *FMR1* trinucleotide expansion, and normal metabolic screening (plasma and urine amino acid chromatography, blood lactate, pyruvate, ketone bodies, uric acid, ammonia, serum transferrin glycosylation, very long chain fatty acids, and urine organic acid chromatography). CNV analysis with the Illumina 1M SNP microarray in the child and his parents[13] revealed the maternally-inherited *GLRA2* deletion; no other clinically-relevant CNVs were detected.

Patient 2: *GLRA2 missense mutation (p.R153Q), de novo*

Patient 2 is a male born preterm at 8 months to non-consanguineous European parents. Both parents were healthy. There was a family history of autism in a sister (see below) and two cousins (second and third degree), descendants of male relatives of the mother. Birth weight was 2,300 g. He presented poor sucking in the newborn period, sat up at 12 months and walked at 18 months. Autism features and hyperactivity were noted at the age of 1 year. He had severe language delay, with first words at 4 years and first phrases at 5 years of age. As an adult he talks a great deal about subjects that interest him without real communication. Generalized tonic-clonic seizures started at the age of 18 years; he is treated with antiepileptic drugs and has about one seizure per year, except for a seizure-free period of several years in his thirties.

He met criteria for autism according to the ADI-R (social: 18, verbal communication: 25, repetitive behaviors: 7, abnormality before age 36 months: 5). Cognitive evaluation with the Wechsler Adult Intelligence Scale (WAIS) at the age of 43 years revealed mild ID: verbal IQ 63, performance IQ 67, full-scale IQ 63. When last evaluated at the age of 45 years, he had no dysmorphic features, his head circumference was 54 cm (-1.5 SD) and the physical exam was normal. He lives by himself in a sheltered home environment and cares for all of his personal needs.

He had normal results for G-banding chromosome analysis at 550-850 band resolution, *FMR1* trinucleotide expansion, and metabolic investigations. No clinically-relevant CNVs were detected with the Illumina Infinium 1M single SNP microarray.[13] Magnetic resonance imaging of the brain was normal.

One of the patient's older sisters has a diagnosis of autism and mild ID. She is more severely affected than her brother; she spoke her first words at 14 months but at 16 months underwent a developmental regression and lost all language until the age of 9 years, when she started to speak in full sentences. Due to behavioral problems she was placed in an institution for the mentally handicapped, where she rapidly regressed and her language deteriorated; after a psychotic episode she spent several years in a psychiatric hospital. She has no history of seizures. The etiological screening performed thus far (karyotype, *FMR1* trinucleotide expansion,

metabolic screening, chromosomal microarray analysis, and brain MRI) has been negative. She does not carry the *GLRA2* mutation (p.R153Q) identified in her brother, indicating intrafamilial genetic heterogeneity, a phenomenon reported in ASD[14-17], and not unexpected given the high frequency of ASD in the general population and the profound etiological heterogeneity underlying autism.

SUPPLEMENTARY FIGURES

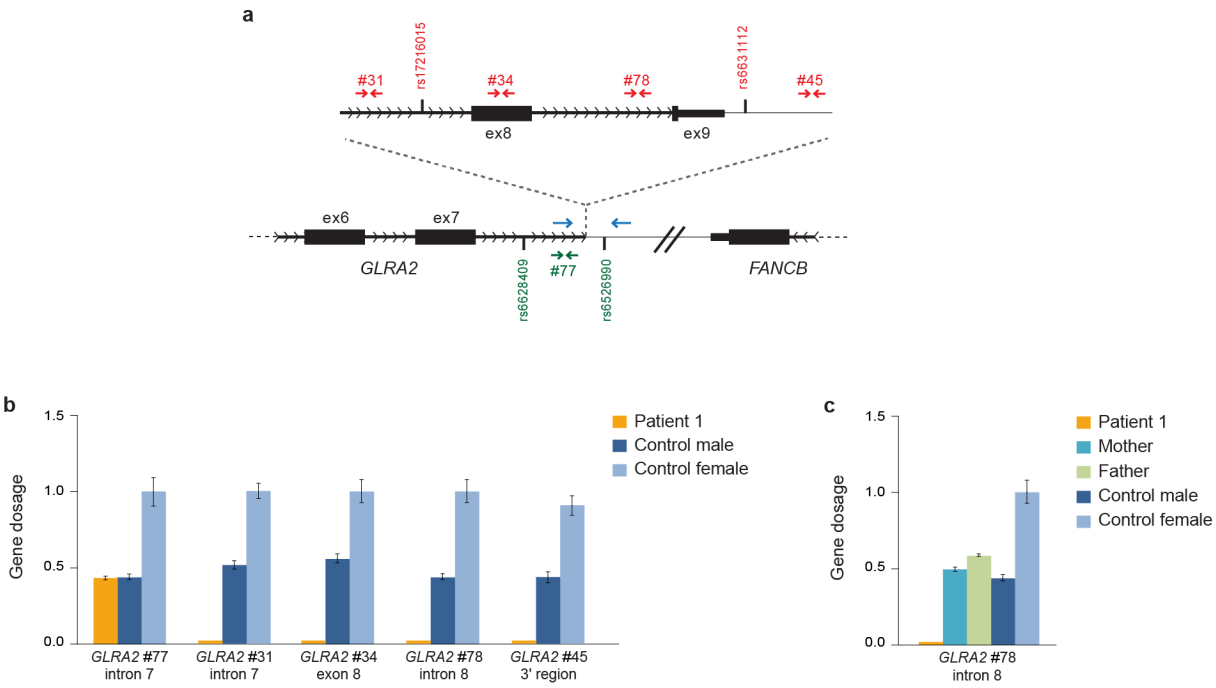

Supplementary Figure S1. Identification and characterization of a microdeletion of *GLRA2* in ASD. (**a**) Schematic representation of the deleted region in Patient 1. Markers rs17216015 to rs6631112, corresponding to the chromosomal region chrX:14,693,216-14,836,199 (hg19), were deleted according to the microarray analysis and are shown in red; the first non-deleted SNPs are shown in green. Specific primers were used to validate and roughly map the deletion by real-time qPCR. Deleted and non-deleted probes are indicated by red and green arrows, respectively, with the qPCR UPL probe numbers. The junction across the deletion was amplified by long-range PCR; the position of the primers is indicated by blue arrows. (**b**) Fluorescent probe-based qPCR using primers shown in (**a**) with the UPL probe numbers confirmed the deletion of exons 8 and 9 of *GLRA2* in Patient 1, compared to primers in intron 7 located outside the deleted region. (**c**) Maternal inheritance of the deletion. The qPCR assay using primers located in the deleted region revealed a gene dosage of 0.5 in the mother of Patient 1, compared to a level of 1 in a control female with two intact X chromosomes, confirming that the mother has one *GLRA2* deleted allele. Data represent mean ± SEM.

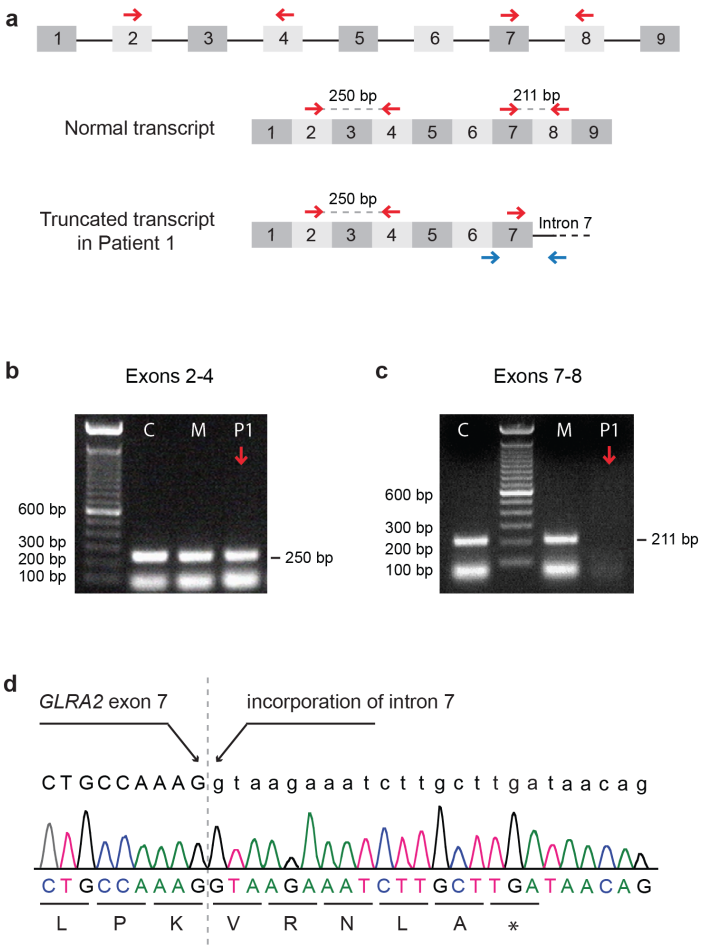

Supplementary Figure S2. Characterization of a truncated transcript in Patient 1. (**a**) Top: Schematic representation of the *GLRA2* gene and position of primers (red arrows) used for cDNA analysis. Middle: Normal cDNA and intron-spanning primers used for RT-PCR with PCR product size. Bottom: Truncated transcript missing exons 8 and 9; the primers used for cDNA sequencing are indicated in blue. (**b**) RT-PCR using primers located in exons 2 and 4 demonstrated the presence of a transcript in Patient 1 (red arrow), suggesting that there is little or no nonsense-mediated mRNA decay. C, control; M, mother of Patient 1; P1, Patient 1. The bands at the bottom of the gel correspond to excess primers. (**c**) No amplification was detected in the patient using primers spanning exons 7 and 8, confirming that the transcript is truncated. In the mother, the non-deleted allele is amplified. (**d**) cDNA sequencing of the *GLRA2* transcript amplified with the primers indicated in blue in (**a**) showed that the deletion of exons 8 and 9 caused the incorporation of intron 7 at the end, leading to a stop codon after six amino acids (VRNLA*).

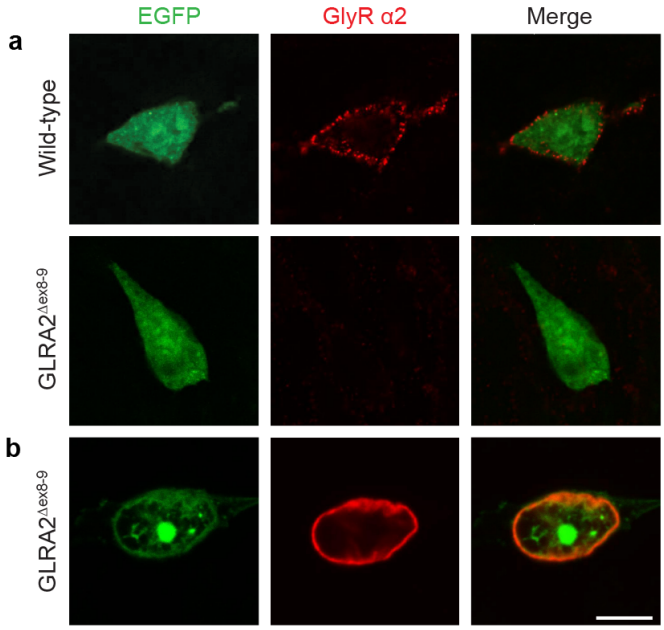

Supplementary Figure S3. The GLRA2 truncated mutant fails to localize properly in transfected CHO cells. Confocal images showing EGFP expression (green) and N-18 staining of the GlyR α2 subunit (red) in transfected CHO cells expressing the wild-type or the truncated mutant (GLRA2$^{\Delta ex8\text{-}9}$). (**a**) Under normal conditions, in non-permeabilized cells, the wild-type GLRA2 protein was expressed at the plasma membrane, whereas no GlyR α2 staining was observed in CHO cells transfected with the GLRA2$^{\Delta ex8\text{-}9}$ construct, as already shown in Figure 2. (**b**) After permeabilization of the cells with Triton X-100, GLRA2$^{\Delta ex8\text{-}9}$ was detected in the cytoplasm, as shown by the N-18 diffuse staining close to the cell surface. Scale bar, 10 µm.

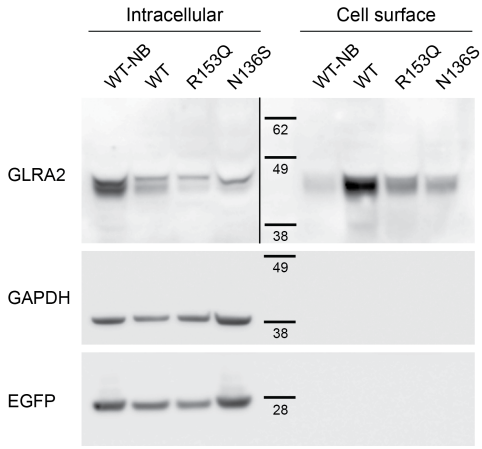

Fraction	WT	R153Q	N136S
Intracellular	6163 (100%)	4200 (68%)	5262 (85%)
Cell surface	17682 (100%)	7719 (44%)	5786 (33%)

Supplementary Figure S4. Cell surface biotinylation analysis of *GLRA2* mutations. Transfected CHO cells were incubated with biotin, and the intracellular and biotinylated cell surface proteins were analyzed by western blot and densitometry. NB, Non-biotinylated control. Two intracellular proteins were used as controls for absence of biotinylation: endogenously expressed GAPDH and co-transfected EGFP. Lanes separated by the vertical line were from the same blot, but were not contiguous in the original gel. The center lane contains molecular size standards. Quantification of intracellular and cell surface expression of wild-type and GLRA2 mutants; values represent optical density, with the percentage of wild-type expression indicated in parentheses. Both GLRA2 mutants showed a markedly reduced cell-surface expression (–56% for GLRA2^{R153Q} and –67% for GLRA2^{N136S}) compared with the wild-type receptor. Intracellular expression was also decreased in both mutants, albeit to a lesser extent. Experiments with cells expressing the wild-type and GLRA2^{R153Q} proteins were repeated twice, with similar findings; the GLRA2^{N136S} mutation was tested only once.

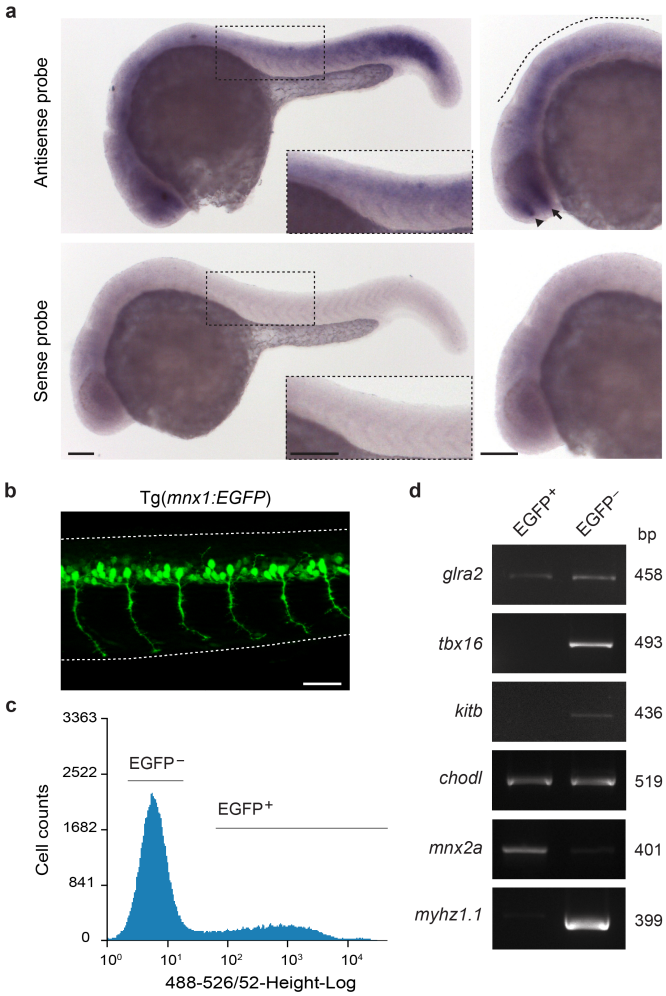

Supplementary Figure S5. *glra2* expression in zebrafish spinal motor neurons. (**a**) Whole-mount *in situ* hybridization with *glra2* antisense and sense riboprobes at 24 hpf. Lateral views of whole-mount embryos (left panels) or of the head (right panels), with anterior to the left. The arrow and arrowhead show *glra2* expression in the ventral and dorsal telencephalon, while the dotted line indicates *glra2* expression in the hindbrain. Insets in left panels are higher magnifications of the boxed regions and show *glra2* expression in the spinal cord. Scale bars, 100 µm. (**b**) Lateral view of the trunk (anterior to the left) of a 24-hpf Tg(*mnx1*:EGFP) embryo showing specific expression of EGFP in spinal motor neurons. Scale bar, 50 µm. Dotted lines delineate the embryonic trunk. (**c**) FAC sorting of EGFP+ spinal motor neurons from 24-hpf Tg(*mnx1*:EGFP) trunks. Fluorescence scatter is used to sort cells according to their fluorescence intensity. The gates used to isolate EGFP+ and EGFP– cells were chosen with a maximum of stringency to avoid cross-contamination of the respective cell populations. (**d**) RT-PCR analysis of *glra2* on EGFP+ and EGFP– cell populations. RT-PCR amplification of transcripts specifically expressed in interneurons (*tbx16*), Rohon-Beard sensory neurons (*kitb*), and muscle cells (*myhz1.1*), or enriched in spinal motor neurons (*chodl* and *mnx2a*), was used to confirm the purity of the EGFP+ cell population.

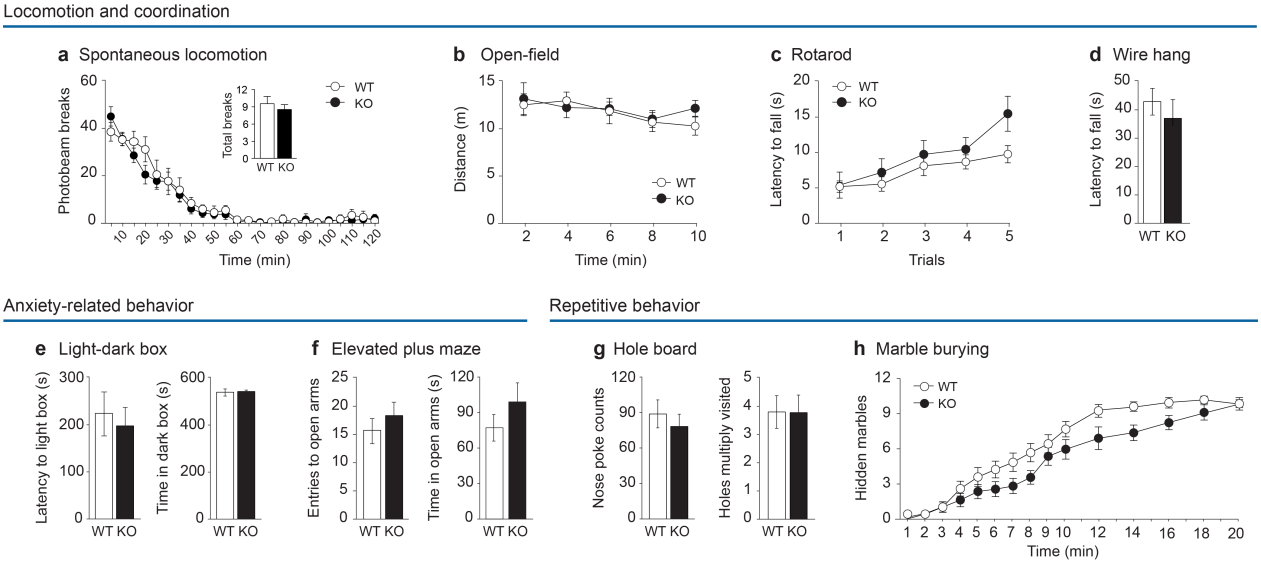

Supplementary Figure S6. *Glra2* mutant mice showed normal locomotion, coordination, anxiety and repetitive behavior. (**a**) Spontaneous locomotion (horizontal and vertical activity) was normal in mutant mice (*n*=13 WT, 15 *Glra2*$^{-/Y}$). No differences were observed between genotypes when analyzing horizontal and vertical activity separately (data not shown). (**b**) Distance travelled in the open-field over a 10 min session was similar between genotypes (*n*=16 WT, 15 *Glra2*$^{-/Y}$). (**d**) *Glra2*$^{-/Y}$ mice showed normal motor coordination on an accelerating rotarod (*n*=11 WT, 8 *Glra2*$^{-/Y}$). (**d**) Mutant mice exhibited normal performance in the wire hang test (*n*=16 WT, 15 *Glra2*$^{-/Y}$). (**e**) Latency to enter the light side and time spent in the dark chamber were comparable between genotypes in the light-dark box test (*n*=16 WT, 15 *Glra2*$^{-/Y}$). (**f**) Number of entries and cumulative time spent in the open arms were normal in *Glra2*$^{-/Y}$ mice in the elevated plus maze (*n*=11 WT, 12 *Glra2*$^{-/Y}$). (**g**) Mutant mice tested in the hole board showed similar nose poke counts and number of holes multiply visited compared to the WT mice (*n*=9 WT, 8 *Glra2*$^{-/Y}$). (**h**) Marble burying did not reflect any repetitive or anxiety-like behavior when quantified by the number of marbles buried during a 20 min test period (*n*=16 WT, 15 *Glra2*$^{-/Y}$).

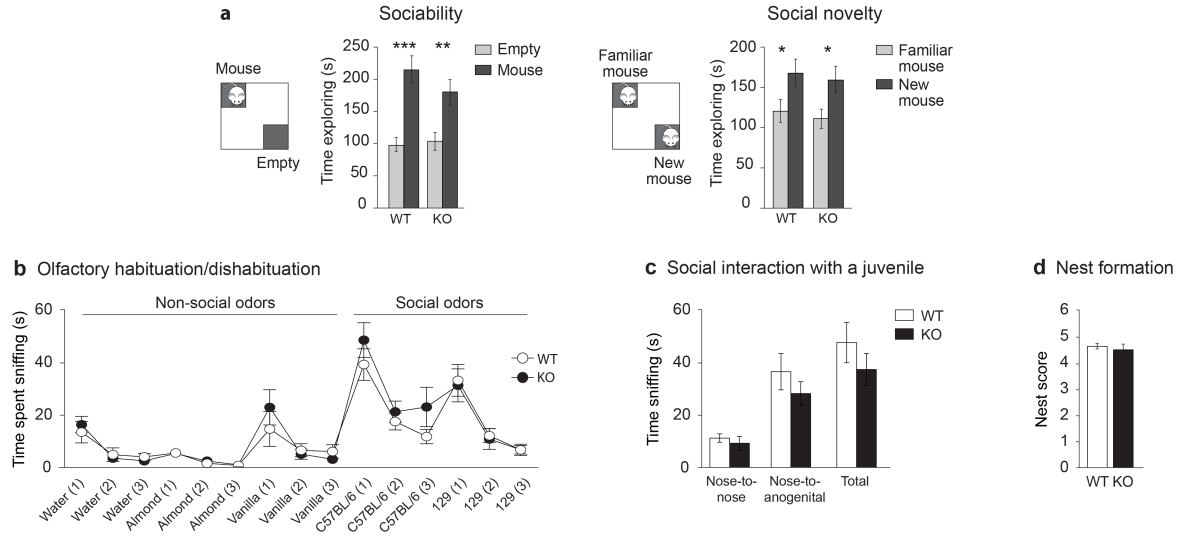

Supplementary Figure S7. *Glra2* mutant mice exhibited normal social behavior. (**a**) During the social approach task, both WT and *Glra2*$^{-/Y}$ showed preference for a caged mouse over an empty box as measured by time spent exploring both cages. In the preference for social novelty task, both genotypes showed normal social memory and preference for a novel stranger mouse (n=36 WT, 38 *Glra*$^{2-/Y}$; data pooled from four cohorts). (**b**) Olfactory habituation and dishabituation to nonsocial and social odors were measured as time spent sniffing odors presented on a series of cotton swabs. No difference was observed between genotypes (*n*=16 WT, 15 *Glra2*$^{-/Y}$). (**c**) Time spent sniffing a male juvenile C57BL/6J was comparable between genotypes (*n*=15 mice/genotype). (**d**) *Glra2*$^{-/Y}$ mice displayed normal quality scores of nest formation (*n*=8 mice/genotype). Data represent mean ± sem. **P*<0.05, ***P*<0.01, ****P*<0.001.

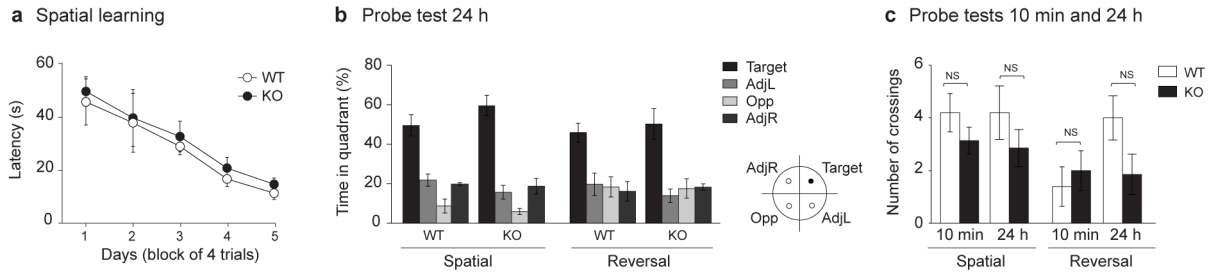

Supplementary Figure S8. *Glra2* mutant mice showed no deficits in the Morris water maze test. (**a**) Mean escape latencies during training in the hidden platform test indicated similar spatial learning in WT and mutant mice (*n*=5 WT, 7 *Glra2*$^{-/Y}$). (**b**) Both genotypes showed a significant preference for the target quadrant during a probe trial performed 10 min (**Figure 4c**) or 24 h after the last training session in the spatial and reversal tasks. (**c**) The number of platform crossings during probe trials (10 min and 24 h) was also similar for both genotypes in the spatial and reversal tests. AdjL, adjacent left quadrant; AdjR, adjacent right quadrant; Target, target quadrant; Opp, opposite to target quadrant. Data represent mean ± sem.

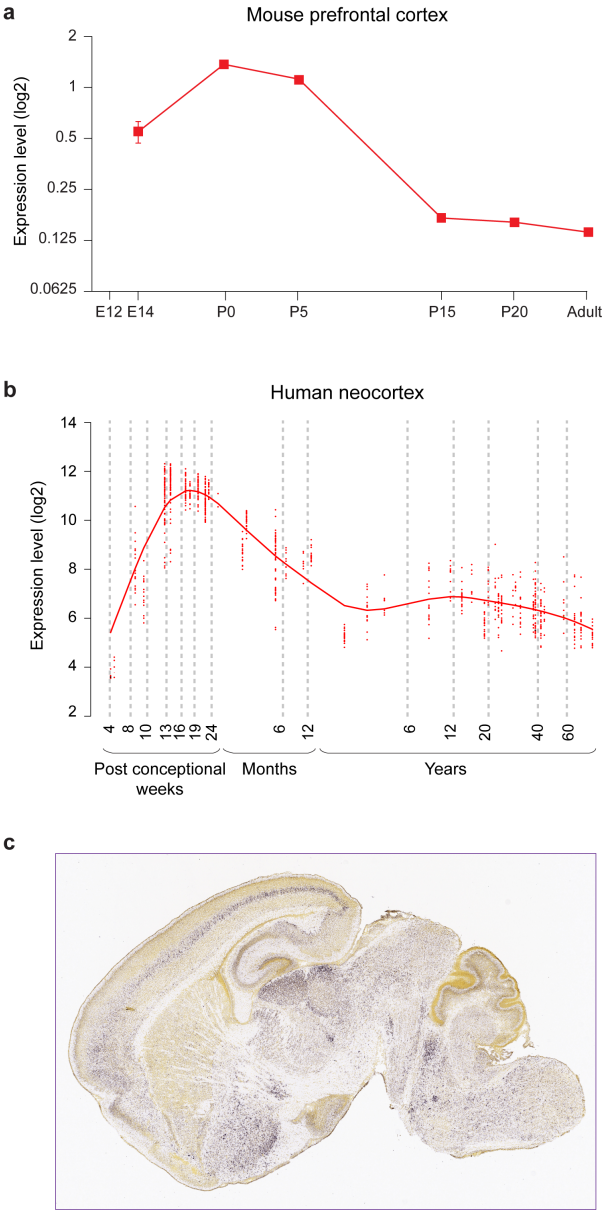

Supplementary Figure S9. Expression of the gene encoding the GlyR α2 subunit in mouse and human brain. (**a**) Real-time reverse transcription PCR on prefrontal cortex mRNAs from wild-type mice showed the relative expression of *Glra2* during embryonic (E12-E14) and postnatal development (P0-adult) (*n*=4-6 mice/developmental stage). No *Glra2* expression was detected at E12. (**b**) The relative expression of the *GLRA2* gene within human cortical areas during pre- and post-natal periods was obtained from the Human Brain Transcriptome database (http://hbatlas.org). (**c**) Coronal slice showing *Glra2 in situ* hybridization from P4 mouse brain atlas (Allen Mouse Brain Atlas, http://www.brain-map.org).

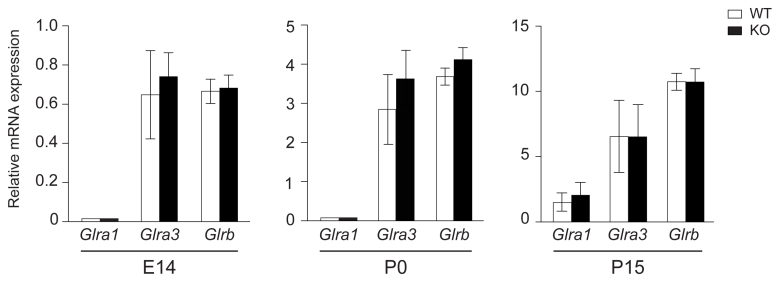

Supplementary Figure S10. mRNA levels of other GlyR subunits in WT and *Glra2*$^{-/Y}$ mice. Real-time reverse transcription PCR of *Glra1*, *Glra3*, and *Glrb* mRNA from prefrontal cortex from WT and *Glra2*$^{-/Y}$ mice showed no evidence for compensatory changes during embryonic (E14) or postnatal development (P0 and P15) (*n*=4 mice per genotype and per developmental stage). *Glra1* expression was only observed at P15. No *Glra4* mRNA was detected in the mouse prefrontal cortex, in agreement with previous findings.[18] Data represent mean ± SEM.

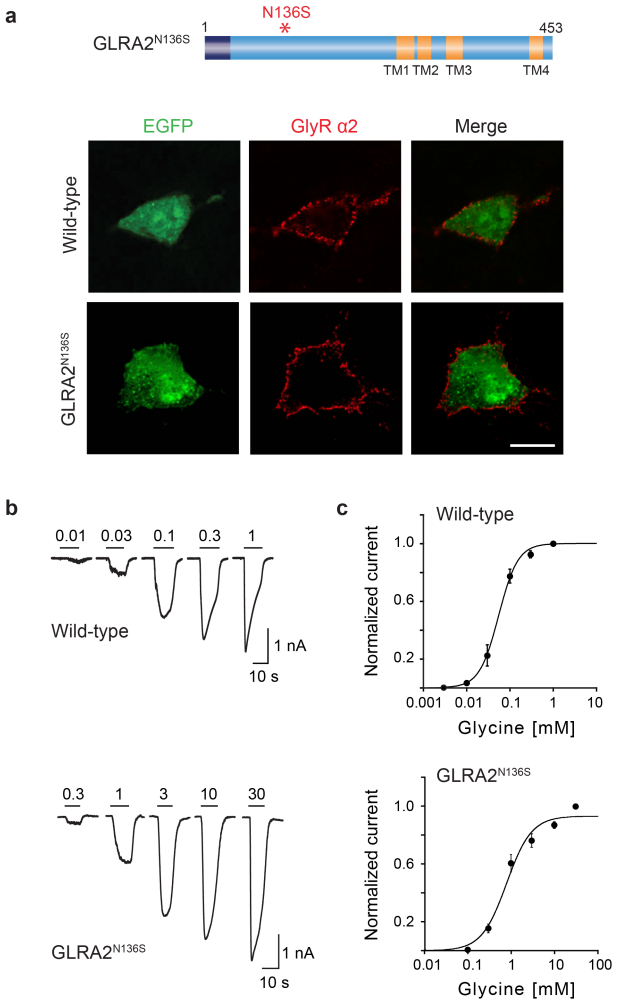

d

Receptor	EC_{50} (mM)	n_H	I_{max} (nA)	n
Wild-type	0.056 ± 0.002	1.96 ± 0.123	2.53 ± 0.34	13
N136S	0.777 ± 0.159*	1.51 ± 0.38	3.44 ± 0.32	8

Supplementary Figure S11. Functional characterization of a second *de novo GLRA2* missense mutation identified in a male with ASD. We characterized a *de novo* missense mutation (c.407A>G, p.N136S) reported recently in a male proband from the Simons Simplex Collection (family ID 11842).[19] The variant was confirmed to be *de novo* and was absent from an unaffected brother. No additional *de novo* variants were identified in the subject. No detailed clinical information is available for this patient. His parents are both Caucasian; in addition to ASD, he has intellectual disability (verbal IQ 15, non-verbal IQ 38).[19] (**a**) Schematic representation of mutated GLRA2 construct co-transfected with EGFP cDNA in CHO cells. The first and last amino acids are numbered; the signal peptide and the four transmembrane domains are shown in dark blue and orange, respectively. The mutation is located in the extracellular binding domain. Confocal cross-sections show surface expression of wild-type and mutant GLRA2 proteins. $GLRA2^{N136S}$ localized properly at the cell surface. Scale bar, 10 µm. (**b**) Representative traces of currents evoked by application of glycine on CHO cells expressing wild-type and mutated GLRA2 proteins. Bars represent application of glycine at concentrations noted. (**c**) Fit of data in (**b**) to the Hill equation. (**d**) Agonist effects of glycine on wild-type and mutant GLRA2. The p.N136S mutation strongly reduced glycine sensitivity (14-fold increase in EC_{50}; *p<0.01, Mann–Whitney U test). Errors indicate SEM. The results of the wild-type construct from Figure 2 are shown again here for comparison.

SUPPLEMENTARY TABLES

Supplementary Table S1. Whole-genome CNV studies including *GLRA2* in ASD and controls

Study	Number of individuals	Details	Reported CNV including *GLRA2*	Method and resolution	Comment	Source
			Controls			
Jakobsson et al. 2008 ([20])	485	485 individuals from the Human Genome Diversity Project–CEPH panel (309 M, 176 F)	No *GLRA2* deletion or duplication	Illumina HumanHap550	Analysis restricted to CNVs >10 SNPs	DGV
Kirov et al. 2009 ([21])	2 792	Schizophrenia study 2 792 controls from the Wellcome Trust Case Control Consortium (1 384 M, 1 408 F)	No *GLRA2* deletion or duplication	Affymetrix 500K	Analysis restricted to CNVs >100 kb	Supp. online
Shaikh et al. 2009 ([22])	2 026	2 026 healthy individuals from the Children's Hospital of Philadelphia, 65% Caucasians (gender not available)	No *GLRA2* deletion; 16 exonic gains	Illumina HumanHap 550	No *GLRA2* duplications have been reported in over 18 000 controls in other studies, suggesting that the gains reported in this study are likely to be artifacts	DGV
Altshuler et al. 2010 ([23])	1 184	1 184 HapMap individuals from 11 populations (gender not available)	No *GLRA2* deletion or duplication	Affymetrix SNP array 6.0, Illumina 1M		DGV
Pinto et al. 2010 ([13]); Pinto et al. 2014 ([24])	9 643	ASD study, Autism Genome Project 4 875 parents and 4 768 controls	***GLRA2* deletion** (chrX:14693216-14836199, hg19) in the mother of 6323-3 (Patient 1)	Illumina 1Mv1, Illumina 1Mv3 Duo	Analysis restricted to CNVs ≥5 kb with ≥5 probes	AGP database
Sanders et al. 2011 ([25])	3 120	ASD study, Simons Simplex Collection 872 unaffected sibs (403 M, 469 F) and 2 248 parents (1 124 M, 1 124 F)	No *GLRA2* deletion or duplication	Illumina 1Mv1, Illumina 1Mv3 Duo		Supp. online
Grond-Ginsbach et al. 2012 ([26])	473	70 cervical artery dissection patients of European ancestry; 403 white Northern Germans collected in the PopGen study	No *GLRA2* deletion or duplication	Affymetrix SNP array 6.0	Analysis restricted to CNVs >100 kb	Supp. online
Silversides et al. 2012 ([27])	756	340 tetralogy of Fallot and/or pulmonary atresia cases of European ancestry; 416 Ontario Population Genomics Platform control individuals	No *GLRA2* deletion or duplication	Affymetrix SNP array 6.0	Analysis restricted to CNVs >10 kb with ≥5 probes	Supp. online
Krepischi et al. 2012 ([28])	168	68 women with breast cancer; 100 controls	No *GLRA2* deletion or duplication	Agilent 180K	Smallest CNV = 7 kb	Supp. online
Total controls	**20 647**					
			ASD cases			
Pinto et al. 2010 ([13]); Pinto et al. 2014 ([24])	2 446	2 446 ASD probands from simplex and multiplex families (Autism Genome Project), including 2 147 European and 299 from other ancestries	***GLRA2* deletion** (chrX:14693216-14836199, hg19) in 6323-3 (Patient 1)	Illumina 1Mv1, Illumina 1Mv3 Duo	Analysis restricted to CNVs ≥5 kb with ≥5 probes	AGP database
Sanders et al. 2011 ([25])	1 124	1 124 ASD probands from simplex families (Simons Simplex Collection)	No *GLRA2* deletion or duplication	Illumina 1Mv1, Illumina 1Mv3 Duo		Supp. online
Total ASD cases	**3 570**					

AGP, Autism Genome Project; ASD, autism spectrum disorder; CNV, copy number variant; DGV, Database of Genomic Variants; F, female; M, male; SNP, single nucleotide polymorphism

Supplementary Table S2. Sequencing of *GLRA2* in controls and cases with ASD or other neurodevelopmental disorders in previous studies

Study	Number of individuals	Males	Females	Approach	Comment
			Controls		
NHLBI Exome Variant Server[a]	6 503 controls	2 443	4 060	Whole exome sequencing	See Supplementary Table S3
1000 Genomes[b]	2 504 controls	1 233	1 271	Whole genome and exome sequencing	13 missense variants also present in the EVS (see Supplementary Table S3); 5 additional missense variants, gender unknown
Klassen *et al.* 2011 ([29])	139 controls	62	77	Targeted sequencing of ion channel genes, including *GLRA2*	
Purcell *et al.* 2014 ([30])	2 543 controls	1 291	1 252	Whole exome sequencing	No rare disruptive or non-synonymous strict variants[c] in *GLRA2*
Total individuals: 11 689 (5 029 males, 6 660 females) Total X chromosomes: 18 349					
			Cases[d]		
Piton *et al.* 2011 ([31])	142 subjects with ASD (122 M, 20 F) and 143 with schizophrenia (95 M, 48 F)	217	68	Targeted sequencing of X-chromosome synaptic genes, including *GLRA2*	One ASD female carries a *GLRA2* missense variant (p.R350L), inherited from a healthy mother (see Supplementary Table S3)
Chahrour *et al.* 2012 ([32])	14 probands with ASD	14		Whole exome sequencing	One ASD male carries a *GLRA2* missense variant (p.I421V), also reported in a male control from the EVS (see Supplementary Table S3)
De Rubeis *et al.* 2014 ([33])	3 871 subjects with ASD	3 150	677	Whole exome sequencing	Gender unknown for 44 samples
Purcell *et al.* 2014 ([30])	2 536 subjects with schizophrenia	1 520	1 016	Whole exome sequencing	No rare disruptive or non-synonymous strict variants[b] in *GLRA2*
Tarpey *et al.* 2009 ([34])	208 families with X-linked intellectual disability, with multiple affected individuals	208	0	Targeted sequencing of X-chromosome coding exons	Two affected males carry a *GLRA2* missense variant (p.I421V), also reported in a male control from the EVS (see Supplementary Table S3)
Rauch *et al.* 2012 ([35])	51 trios with sporadic non-syndromic intellectual disability	19	32	Whole exome sequencing	
De Ligt *et al.* 2012 ([36])	100 trios with intellectual disability	47	53	Whole exome sequencing	
Klassen *et al.* 2011 ([29])	151 subjects with idiopathic epilepsy	66	85	Targeted sequencing of ion channel genes, including *GLRA2*	
Feng *et al.* 2001 ([37])	5 patients with ASD, 113 with schizophrenia, 30 with ADHD	N/A	N/A	Targeted sequencing of *GLRA2*	
Total individuals: 7 364 (5 241 males, 1 931 females and 192 of unknown gender) 4 032 ASD, 2 792 schizophrenia, 359 ID, 151 epilepsy, 30 ADHD					

We searched the p.R153Q mutation and other nonsynonymous variants in *GLRA2* in controls and cases with ASD or other neurodevelopmental disorders in public databases and published studies.

[a] Exome Variant Server, National Heart, Lung, and Blood Institute (NHLBI) GO Exome Sequencing Project (ESP), Seattle, WA (http://evs.gs.washington.edu/EVS/), accessed December 2014, EVS data release ESP6500SI-V2.

[b] 1000 Genomes (http://www.1000genomes.org/), accessed October 2014

[c] In Purcell et al.,[30] disruptive variants are defined as nonsense, essential splice site and frameshift variants; non-synonymous strict variants are predicted to be damaging by five algorithms (PolyPhen2 HumDiv and HumVar, LRT, MutationTaster and SIFT). The *GLRA2* mutation p.R153Q identified in Patient 2 is a non-synonymous strict variant.

[d] Except for two *de novo GLRA2* missense variants in a male and a female with ASD reported by Iossifov *et al.*[19,38] (see Supplementary Table S3), whole-exome sequencing in 2 508 ASD probands (2 167 males, 341 females) and 1 911 unaffected siblings (900 males, 1 011 females) from the Simons Simplex Collection failed to identify other *de novo* variants in *GLRA2*;[19,38-40] however, because these studies only reported *de novo* variants they were not included in this table.

ADHD, attention deficit hyperactivity disorder; ASD, autism spectrum disorder; EVS, Exome Variant Server; F, female; M, male; N/A, not available; NHLBI, National Heart, Lung, and Blood Institute

Supplementary Table S3. Loss-of-function and non-synonymous missense variants reported in *GLRA2* in ASD and in the Exome Variant Server

Variant pos (hg19)	rs number	Variant type	cDNA change	Protein change	Grantham score[a]	GERP[b]	ConSurf[c]	PolyPhen-2[d]	SNPs&GO[e]	MutPred[f]	PANTHER[g]	SIFT[h]	Comment
Variant identified in Patient 2 (this study)													
X:14599492		Missense	c.458G>A	p.R153Q	43	5.64	**9 (e,f)**	**Probably damaging**	**Disease (RI=8)**	**0.896**	**-3.33132**	**Damaging**	Not found in 2443 males and 4060 females from EVS nor reported in the literature
Variants reported in ASD not present in the Exome Variant Server													
X:14548195		Missense	c.16G>C	p.V6L	32	5.47	3 (b)	Possibly damaging	Neutral (RI=2)	0.383	N/A	Tolerated	1 heterozygous ASD female (family ID 12724) among 343 families, *de novo*[38]
X:14599441		Missense	c.407A>G	p.N136S	46	5.64	**9 (e,f)**	**Probably damaging**	**Disease (RI=8)**	**0.913**	**-4.86979**	**Damaging**	1 ASD male (family ID 11842) among 2 508 patients, *de novo*[19]
X:14708950		Missense	c.1049G>T	p.R350L	**102**	5.0	3 (e)	**Probably damaging**	**Disease (RI=6)**	**0.502**	**-3.29768**	**Damaging**	1 heterozygous ASD female among 142 patients (122 males, 20 females), inherited from an unaffected mother[31]
Variants reported in the Exome Variant Server													
X:14550363	rs144675165	Missense	c.71C>T	p.T24M	81	3.98	1 (b)	Benign	Neutral (RI=2)	0.393	N/A	Tolerated	1 heterozygous female out of 4060 1 male out of 2443
X:14550374	rs138307435	Missense	c.82A>G	p.K28E	56	4.87	1 (e)	Possibly damaging	Neutral (RI=1)	0.422	N/A	Tolerated	1 heterozygous female out of 4060 not found in 2443 males
X:14550384	rs376108175	Missense	c.92A>T	p.D31V	**152**	4.87	1 (e)	Possibly damaging	Neutral (RI=4)	0.336	N/A	Tolerated	1 heterozygous female out of 4060 not found in 2443 males
X:14592469	rs374274759	Missense	c.217G>A	p.V73I	29	5.75	**8 (b)**	**Probably damaging**	**Disease (RI=1)**	**0.686**	-1.87838	Tolerated	1 heterozygous female out of 4060 not found in 2443 males
X:14625372	rs372099149	Missense	c.697A>G	p.T233A	58	5.41	**7 (e)**	**Probably damaging**	Neutral (RI=2)	0.443	N/A	Tolerated	1 heterozygous female out of 4060 not found in 2443 males
X:14627133	rs369673191	Missense	c.736G>A	p.V246I	29	5.83	**7 (b)**	Possibly damaging	Neutral (RI=5)	0.469	-1.65239	Tolerated	1 heterozygous female out of 4060 not found in 2443 males
X:14708965	rs150064102	Missense	c.1064A>G	p.Q355R	43	5.0	3 (e)	Possibly damaging	Neutral (RI=9)	0.295	-0.29526	Tolerated	1 heterozygous female out of 4060 not found in 2443 males
X:14748420	rs144022438	Missense	c.1172C>T	p.A391V	64	3.73	1 (e)	Benign	Neutral (RI=6)	0.489	-1.50148	Tolerated	12 heterozygous females out of 4060 2 males out of 2443
X:14748434	rs368138282	Missense	c.1186C>A	p.P396T	38	5.5	1 (e)	Benign	Neutral (RI=8)	0.350	-0.91321	Tolerated	1 heterozygous female out of 4060 not found in 2443 males
X:14748441	rs146448798	Missense	c.1193C>T	p.P398L	98	4.63	1 (e)	Possibly damaging	Neutral (RI=7)	0.385	-1.28414	Tolerated	3 heterozygous females out of 4060 not found in 2443 males
X:14748447	rs370575329	Missense	c.1199C>T	p.P400L	98	4.63	1 (e)	Possibly damaging	Neutral (RI=7)	0.423	-1.2556	Tolerated	1 heterozygous female out of 4060 not found in 2443 males
X:14748507	rs140931950	Missense	c.1259C>T	p.T420M	81	5.5	**6 (e)**	**Probably damaging**	**Disease (RI=1)**	0.392	**-3.00602**	Tolerated	1 heterozygous female out of 4060 not found in 2443 males
X:14748509	rs200619146	Missense	c.1261A>G	p.I421V	29	4.32	4 (b)	Benign	Neutral (RI=7)	**0.566**	-0.99275	Tolerated	1 heterozygous female out of 4060 1 male out of 2443

An extensive search for nonsense, frameshift, splice-site, and non-synonymous missense variants in *GLRA2* was conducted using data from the Exome Variant Server (EVS) (http://evs.gs.washington.edu/EVS/, accessed December 2014) and from the literature. Our patient and an affected male from the Simons Simplex Collection[19] are the only two males carrying mutations predicted to be deleterious by PolyPhen-2, SNPs&GO, MutPred, PANTHER, and SIFT. In addition, the mutated residues are highly conserved (high GERP and ConSurf scores) and are the only ones predicted to be functional ("f") by Consurf.

[a] The Grantham score measures the degree of amino acid substitution;[41] closely similar pairs have scores <60, strongly dissimilar pairs have scores >100.

[b] GERP positive scores represent a substitution deficit and thus indicate that a site may be under evolutionary constraint.[42] Scores range from 6.18 to –12.36; scores >2 indicate likely truly constrained sites.

[c] ConSurf calculates the evolutionary conservation of amino acid positions;[43] the conservation scores range from 1 to 9, with 9 corresponding to highly conserved residues; residue position/function scores: e = exposed residue, b = buried residue, f = functional residue (highly conserved and exposed), s = structural residue (highly conserved and buried).

[d] PolyPhen-2 classifies the functional effect of missense variants into three categories: probably damaging, possibly damaging, and benign; variants were assessed using the HumDiv-trained model.[44]

[e] SNPs&GO classifies the effect of variants as neutral or disease-related; the reliability index (RI) of the prediction ranges from 0 (unreliable) to 10 (reliable).[45]

[f] MutPred classifies amino acid substitution as disease-associated (p >0.5) or neutral (p <0.5).[46]

[g] PANTHER estimates the likelihood of a particular non-synonymous coding SNP to cause a functional impact on the protein.[47] The substitution score (subPSEC) ranges from 0 to about –10; 0 implies a functionally neutral change whereas more negative scores predict more deleterious substitutions; a subPSEC < –3 has been suggested as a useful cutoff value.

[h] SIFT predicts whether an amino acid substitution affects protein function based on sequence homology and the physical properties of amino acids and classifies variants into two categories, damaging or tolerated.[48]

Supplementary Table S4. Sequence variants identified in the *GLRA2* gene in 400 patients with ASD

Nucleotide change	rs number	Variant type	Amino acid change	Location	Frequency in male patients (n=400)
c.203-24C>T		Intronic	–	Intron 2	T=1/C=399
c.271-75A>G	rs2074210	Intronic	–	Intron 3	G=188/A=212
c.271-43G>A	rs370972754	Intronic	–	Intron 3	A=1/G=399
c.285T>C		Silent	p.N95=	Exon 4	C=1/T=399
c.458G>A		**Missense**	**p.R153Q**	**Exon 4**	**A=1/G=399**
c.494+44A>G	rs2074211	Intronic	–	Intron 4	G=221/A=179
c.501C>A		Silent	p.T167=	Exon 5	A=1/C=399
c.507C>T	rs111946619	Silent	p.T169=	Exon 5	T=11/C=389
c.931-19_931-18insTCTC		Intronic	–	Intron 7	CTCTC=2/C=398
c.931-33_931-32insTG		Intronic	–	Intron 7	CTG=1/C=399
c.747C>T	rs2229963	Silent	p.H249=	Exon 7	T=112/C=288
c.1089C>T	rs78179793	Silent	p.D363=	Exon 9	T=2/C=398

The mutation in Patient 2 is indicated in bold.

Supplementary Table S5. Agonist effects of glycine on wild-type and mutant GLRA2

Receptor	EC_{50} (mM)	n_H	I_{max} (nA)	*n*
Wild type	0.056 ± 0.002	1.96 ± 0.123	2.53 ± 0.34	13
R153Q	8.9 ± 0.9[a]	1.35 ± 0.1	2.31 ± 0.49	7

[a] $p<0.01$, mutant versus wild-type, Mann–Whitney U test

Supplementary Table S6. Statistical analyses

Zebrafish experiments					
Experiment	# of embryos	Parameter	Statistical test	Significance	Figure
Morphants	8–15 (3 experiments)	Number of branches	Student's t-test, unequal variance	Control vs $MO^{\alpha 2}$: p<0.0001	—
Rescue WT	8–15 (4 experiments)	Number of branches	Student's t-test	Control vs $MO^{\alpha 2}$: p=0.003 $MO^{\alpha 2}$ vs ($MO^{\alpha 2}$ + $mRNA^{\alpha 2}$): p=0.014 Control vs ($MO^{\alpha 2}$ + $mRNA^{\alpha 2}$): p=0.91	Fig. 3
Rescue mutation (R153Q)	8–15 (4 experiments)	Number of branches	Student's t-test	Control vs $MO^{\alpha 2}$: p=0.0009 $MO^{\alpha 2}$ vs ($MO^{\alpha 2}$ + $mRNA^{\alpha 2R153Q}$): p=1.00 Control vs ($MO^{\alpha 2}$ + $mRNA^{\alpha 2R153Q}$): p=0.0006	
Rescue deletion	8 (4 experiments)	Number of branches	Student's t-test, unequal variance	Control vs $MO^{\alpha 2}$: p<0.0001 $MO^{\alpha 2}$ vs ($MO^{\alpha 2}$ + $mRNA^{\alpha 2del}$): p=0.48 Control vs ($MO^{\alpha 2}$ + $mRNA^{\alpha 2del}$): p=0.024	
Behavioral experiments					
Test	# of mice	Parameter	Statistical test	Significance	Figure
Spontaneous locomotion	WT = 13 KO = 15	Total locomotor activity (horizontal plus vertical) (photobeam breaks)	Mann-Whitney U test	p=0.66	Fig. S6a
		Horizontal activity (photobeam breaks)	Mann-Whitney U test	p=0.63	—
		Vertical activity (photobeam breaks)	Mann-Whitney U test	p=0.87	—
Open field	WT = 16 KO = 15	Distance (m)	Two-way ANOVA	Genotype, $F_{(1,29)}$=0.17, p=0.69 Time, $F_{(4,116)}$=2.24, p=0.07 Genotype x Time, $F_{(4,116)}$=0.66, p=0.62	Fig. S6b
		Total distance (m)	Student's t-test	p=0.69	—
Rotarod	WT = 11 KO = 8	Latency to fall (s)	Two-way ANOVA (after square root transformation)	Genotype, $F_{(1,17)}$=1.29, p=0.27 Trial, $F_{(4,68)}$=12.29, p<0.0001 Genotype x Trial, $F_{(4,68)}$=1.16, p=0.34	Fig. S6c
Wire hang	WT = 16 KO = 15	Latency to fall (s)	Mann-Whitney U test	p=0.64	Fig. S6d
Light-dark box	WT = 16 KO = 15	Number of transitions	Mann-Whitney U test	p=0.78	—
		Time in dark box (s)	Mann-Whitney U test	p=0.68	Fig. S6e
		Latency to light box (s)	Mann-Whitney U test	p=0.89	
Elevated plus maze	WT = 11 KO = 12	Time in open arms (s)	Student's t-test	p=0.26	Fig. S6f
		Entries to open arms	Student's t-test	p=0.48	
Hole board	WT = 9 KO = 8	Nose poke counts	Student's t-test	p=0.52	Fig. S6g
		Holes multiply visited	Student's t-test	p=0.97	
Marble burying	WT = 16 KO = 15	Hidden marbles	Two-way ANOVA	Genotype, $F_{(1,29)}$=3.77, p=0.06 Time, $F_{(14,406)}$=136.53, p<0.0001 Genotype x Time, $F_{(14,406)}$=2.06, p=0.01	Fig. S6h
Sociability and preference for social novelty	WT = 36 KO = 38 (4 pooled cohorts)	Time exploring (s) Sociability	Mann-Whitney U test	WT (empty vs stranger 1): p<0.0001 KO (empty vs stranger 1): p=0.003	Fig. S7a
		Time exploring (s) Social novelty	Mann-Whitney U test	WT (stranger 2 vs stranger 1): p=0.03 KO (stranger 2 vs stranger 1): p=0.04	
Olfactory habituation/dishabituation	WT = 16 KO = 15	Time spent sniffing (s)	Two-way ANOVA (after log transformation)	Genotype, $F_{(1,29)}$=0.41, p=0.53 Trial, $F_{(14,406)}$=30.06, p<0.0001 Genotype x Trial, $F_{(14,406)}$=0.71, p=0.76	Fig. S7b

Test	# of mice	Parameter	Statistical test	Significance	Figure
Social interaction with a juvenile	WT = 8 KO = 7	Time sniffing nose-to-nose (s)	Mann-Whitney U test	p=0.28	Fig. S7c
		Time sniffing nose-to-anogenital (s)	Mann-Whitney U test	p=0.46	
		Total time sniffing (s)	Mann-Whitney U test	p=0.54	
Nest formation	WT = 8 KO = 8	Nest score	Mann-Whitney U test	p=0.91	Fig. S7d
Novel object recognition	WT = 11 KO = 12	Exploration time (s) Probe test 10 min	Mann-Whitney U test	WT (novel vs familiar): p=0.0003 KO (novel vs familiar): p=0.06	Fig. 4a
		Discrimination index Probe test 10 min	Mann-Whitney U test	p=0.025	
	WT = 16 KO = 15	Exploration time (s) Probe test 24 h	Mann-Whitney U test	WT (novel vs familiar): p=0.023 KO (novel vs familiar): p=0.74	
		Discrimination index Probe test 24 h	Mann-Whitney U test	p=0.026	
Novel location recognition	WT = 9 KO = 10	Exploration time (s) Probe test 10 min	Mann-Whitney U test	WT (novel vs familiar): p=0.006 KO (novel vs familiar): p=0.012	Fig. 4b
		Discrimination index Probe test 10 min	Mann-Whitney U test	p=0.40	
Morris water maze Cued version	WT = 5 KO = 7	Escape latency (s)	Two-way ANOVA (log transformed data)	Genotype, $F_{(1,10)}$=0.13, p=0.72 Trial, $F_{(15,150)}$=19.02, p<0.0001 Genotype x Trial, $F_{(15,150)}$=0.85, p=0.62	—
Morris water maze Spatial learning	WT = 5 KO = 7	Escape latency (s) Training	Two-way ANOVA (log transformed data)	Genotype, $F_{(1,10)}$=0.44, p=0.52 Day, $F_{(4,40)}$=11.53, p<0.0001 Genotype x Day, $F_{(4,40)}$=0.11, p=0.98	Fig. S8a
		Time in quadrant (s) Probe test 10 min	Two-way ANOVA (log transformed data)	Genotype, $F_{(1,10)}$=0.48, p=0.51 Quadrant, $F_{(3,30)}$=29.30, p<0.0001 Genotype x Quadrant, $F_{(3,30)}$=0.67, p=0.58	Fig. 4c
		Platform crossing Probe test 10 min	Student's t-test (log transformed data)	p=0.29	Fig. S8c
		Escape latency (s) Probe test 10 min	Student's t-test (log transformed data)	p=0.27	—
		Time in quadrant (s) Probe test 24 h	Two-way ANOVA (log transformed data)	Genotype, $F_{(1,10)}$=1.05, p=0.33 Quadrant, $F_{(3,30)}$=19.70, p<0.0001 Genotype x Quadrant, $F_{(3,30)}$=0.35, p=0.79	Fig. S8b
		Platform crossing Probe test 24 h	Student's t-test (log transformed data)	p=0.28	Fig. S8c
		Escape latency (s) Probe test 24 h	Student's t-test (log transformed data)	p=0.49	—
Morris water maze Spatial reversal learning	WT = 5 KO = 7	Escape latency (s) Training	Two-way ANOVA (log transformed data)	Genotype, $F_{(1,10)}$=0.35, p=0.57 Trial, $F_{(7,70)}$=3.55, p=0.003 Genotype x Trial, $F_{(7,70)}$=1.11, p=0.36	—
		Time in quadrant (s) Probe test 10 min	Two-way ANOVA (log transformed data)	Genotype, $F_{(1,10)}$=0.001, p=0.97 Quadrant, $F_{(3,30)}$=5.83, p=0.003 Genotype x Quadrant, $F_{(3,30)}$=1.24, p=0.31	Fig. 4c
		Platform crossing Probe test 10 min	Student's t-test (log transformed data)	p=0.53	Fig. S8c
		Escape latency (s) Probe test 10 min	Student's t-test (log transformed data)	p=0.90	—

Test	# of mice	Parameter	Statistical test	Significance	Figure
Morris water maze Spatial reversal learning	WT = 5 KO = 7	Time in quadrant (s) Probe test 24 h	Two-way ANOVA (log transformed data)	Genotype, $F_{(1,10)}$=0.02, p=0.88 Quadrant, $F_{(3,30)}$=5.46, p=0.004 Genotype x Quadrant, $F_{(3,30)}$=0.31, p=0.82	Fig. S8b
		Platform crossing Probe test 24 h	Student's t-test (log transformed data)	p=0.09	Fig. S8c
		Escape latency (s) Probe test 24 h	Student's t-test (log transformed data)	p=0.12	—

***Ex vivo* electrophysiology**

Experiment	# of slices	Parameter	Statistical test	Significance	Figure
Long-term potentiation	WT = 14 KO = 10	Field excitatory postsynaptic potentials (% baseline)	Wilcoxon's signed ranks test	WT (basal vs last 10 min): p=0.0002 KO (basal vs last 10 min): p=0.36	Fig. 4d

Supplementary Table S7. Primers used for *GLRA2* sequencing and cDNA analysis

Primer	Sequence (5'-3')	Product size (bp)
***GLRA2* sequencing**		
Exon1-F	TCGGGATATTTTCCACAAGC	188
Exon1-R	TCCAGAGCACAGATAAATACACAA	
Exon2-F	GCGTTAGCTCTCAAGGGATG	237
Exon2-R	GAAGATTTCTCAAAGGCTTAACG	
Exon3-F	TCTAGCCAATTGCACAGATGTT	555
Exon3-R	CAGAAAACCATTAAAACATCAAATG	
Exon4-F	TTCTCCCTTTTGTCCCCTCT	517
Exon4-R	AAACAAGAAACCACAAAAGTCAAA	
Exon5-F	GCCCTGAGTTGGAGCTTAGA	350
Exon5-R	CATTAGGATGTTGGGGGTTG	
Exon6-F	TGACTGAGCGTATGTCTGCTTT	357
Exon6-R	GCCTGGTAAATATGCAGCAA	
Exon7-F	TGGTTCAGTTGGAGAAGAGTTG	523
Exon7-R	CAGCTTCTTGTCCTCTTATTGC	
Exon8-F	GGTTATTTTGCTGCTCACACC	360
Exon8-R	GGCTTCTTGCTTATTGTGTGC	
Exon9-F	TCTGTTCCATGAATAATTGAGTTG	555
Exon9-R	CCCTCCCTCAATCTTCTCCT	
GLRA2 cDNA analysis		
Exon2-F	GATGCAAGAATCAGGCCAAA	250
Exon4-R	AGTTGGCACCCTTCTCATTG	
Exon7-F	TTTTGTCCTGGGTTTCCTTT	211
Exon8-R	AAGTTCACCGCTGCGTATTC	
Ex6-7-F	CAACACTGGAAAGTTTACCTGC	371
Intron7-R	TCTCAAACTCAGCTTCTTGTCC	

Supplementary Table S8. Primers used for real-time RT-PCR of GlyR subunits in the mouse prefrontal cortex

Primer	Sequence (5'-3')	UPL probe number
Glra1-38F	TGGGAGACCATTGTATTCTTCA	#38
Glra1-38R	GGAAGTCCGAGGGTGACATA	
Glra1-74F	GTTCCATCGCTGAGACAACC	#74
Glra1-74R	GGGTATTCATTGTAGGCCAGAC	
Glra2-85F	TTAGGGACAAACCACTTCAGG	#85
Glra2-85R	GGTCTGCGAGGGATGTTTT	
Glra2-53F	GACTACACAGAGTTCAGGTTCCAG	#53
Glra2-53R	TCCAGATGTCAATTGCTTTCA	
Glra3-45F	TCAAGAATTTCCCAATGGATG	#45
Glra3-45R	GGCAAAGTGAGTCCTTCAGC	
Glra3-75F	TTGCGGTACTGCACTAAACACT	#75
Glra3-75R	TCCAGAATGAGACCCAGGAT	
Glra4-81F	TCCTCACCATGACAACTCAGA	#81
Glra4-81R	TGTCAATTGCCTTTACGTAGGA	
Glrb-42F	TGATGCTAGTGCTGCCAGAG	#42
Glrb-42R	GAGCAGGCAGGCAATGAG	
Glrb-66F	AACTCCACCAGCAATATCTTGAA	#66
Glrb-66R	TTGACTACTACATCAACAGGAATGC	
Control gene		
Gusb-31F	GAGGATCAACAGTGCCCATT	#31
Gusb-31R	AGCCTCAAAGGGGAGGTG	

Supplementary Table S9. Primers used for RT-PCR analysis on FAC-sorted zebrafish spinal motor neurons

Primer	Sequence (5'-3')	Product size (bp)
zGlra2_ex2-3-F zGlra2_ex5-6-R	TCTGTACAGCATCAGGCTGACG AGGAGACCTTTGGCAGTGATGC	458
zChodl-F zChodl-R	CTCGCTGTTCAGAAACTGGTATGC TGCTAGCAGGAAGGTGCAGACG	519
zMnx2a-F zMnx2a-R	TCATGCTGACTGAGACACAGG GACACGCAGACTAAAGTAGCC	401
zMyhz1.1-F zMyhz1.1-R	AACTGGAGTCAAGAGTTCGTGAGC GAGGTGTGCTGAAGCAGGTTCC	399
zTbx16-F zTbx16-R	CCGTACAGATTTCACGAATACG AATGGTCTCTCAATCGGTGTCC	493
zKitb-F zKitb-R	CCTGAGAGGAAATGCACGTCTG TGCTGAGATTCAAGTAATCCTGC	436

References

1. Gong X, Bacchelli E, Blasi F, Toma C, Betancur C, Chaste P *et al.* Analysis of X chromosome inactivation in autism spectrum disorders. *Am J Med Genet B Neuropsychiatr Genet* 2008; **147B:** 830-835.
2. Kimmel CB, Ballard WW, Kimmel SR, Ullmann B, Schilling TF. Stages of embryonic development of the zebrafish. *Dev Dyn* 1995; **203:** 253-310.
3. Fassier C, Hutt JA, Scholpp S, Lumsden A, Giros B, Nothias F *et al.* Zebrafish atlastin controls motility and spinal motor axon architecture via inhibition of the BMP pathway. *Nat Neurosci* 2010; **13:** 1380-1387.
4. Macdonald R, Xu Q, Barth KA, Mikkola I, Holder N, Fjose A *et al.* Regulatory gene expression boundaries demarcate sites of neuronal differentiation in the embryonic zebrafish forebrain. *Neuron* 1994; **13:** 1039-1053.
5. Flanagan-Steet H, Fox MA, Meyer D, Sanes JR. Neuromuscular synapses can form in vivo by incorporation of initially aneural postsynaptic specializations. *Development* 2005; **132:** 4471-4481.
6. O'Gorman S, Dagenais NA, Qian M, Marchuk Y. Protamine-Cre recombinase transgenes efficiently recombine target sequences in the male germ line of mice, but not in embryonic stem cells. *Proc Natl Acad Sci USA* 1997; **94:** 14602-14607.
7. Kamei J, Matsunawa Y, Miyata S, Tanaka S, Saitoh A. Effects of nociceptin on the exploratory behavior of mice in the hole-board test. *Eur J Pharmacol* 2004; **489:** 77-87.
8. Moy SS, Nadler JJ, Perez A, Barbaro RP, Johns JM, Magnuson TR *et al.* Sociability and preference for social novelty in five inbred strains: an approach to assess autistic-like behavior in mice. *Genes Brain Behav* 2004; **3:** 287-302.
9. Silverman JL, Turner SM, Barkan CL, Tolu SS, Saxena R, Hung AY *et al.* Sociability and motor functions in Shank1 mutant mice. *Brain Res* 2011; **1380:** 120-137.
10. Deacon RM. Assessing nest building in mice. *Nat Protoc* 2006; **1:** 1117-1119.
11. Altafaj X, Dierssen M, Baamonde C, Marti E, Visa J, Guimera J *et al.* Neurodevelopmental delay, motor abnormalities and cognitive deficits in transgenic mice overexpressing Dyrk1A (minibrain), a murine model of Down's syndrome. *Hum Mol Genet* 2001; **10:** 1915-1923.
12. Chan CS, Weeber EJ, Kurup S, Sweatt JD, Davis RL. Integrin requirement for hippocampal synaptic plasticity and spatial memory. *J Neurosci* 2003; **23:** 7107-7116.
13. Pinto D, Pagnamenta AT, Klei L, Anney R, Merico D, Regan R *et al.* Functional impact of global rare copy number variation in autism spectrum disorders. *Nature* 2010; **466:** 368-372.
14. Szatmari P, Paterson AD, Zwaigenbaum L, Roberts W, Brian J, Liu XQ *et al.* Mapping autism risk loci using genetic linkage and chromosomal rearrangements. *Nat Genet* 2007; **39:** 319-328.
15. Weiss LA, Shen Y, Korn JM, Arking DE, Miller DT, Fossdal R *et al.* Association between microdeletion and microduplication at 16p11.2 and autism. *N Engl J Med* 2008; **358:** 667-675.
16. Tabet AC, Pilorge M, Delorme R, Amsellem F, Pinard JM, Leboyer M *et al.* Autism multiplex family with 16p11.2p12.2 microduplication syndrome in monozygotic twins and distal 16p11.2 deletion in their brother. *Eur J Hum Genet* 2012; **20:** 540-546.
17. Yuen RK, Thiruvahindrapuram B, Merico D, Walker S, Tammimies K, Hoang N *et al.* Whole-genome sequencing of quartet families with autism spectrum disorder. *Nat Med* 2015; **21:** 185-191.
18. Harvey RJ, Schmieden V, Von Holst A, Laube B, Rohrer H, Betz H. Glycine receptors containing the alpha4 subunit in the embryonic sympathetic nervous system, spinal cord and male genital ridge. *Eur J Neurosci* 2000; **12:** 994-1001.
19. Iossifov I, O'Roak BJ, Sanders SJ, Ronemus M, Krumm N, Levy D *et al.* The contribution of de novo coding mutations to autism spectrum disorder. *Nature* 2014; **515:** 216-221.
20. Jakobsson M, Scholz SW, Scheet P, Gibbs JR, VanLiere JM, Fung HC *et al.* Genotype, haplotype and copy-number variation in worldwide human populations. *Nature* 2008; **451:** 998-1003.

21. Kirov G, Grozeva D, Norton N, Ivanov D, Mantripragada KK, Holmans P *et al.* Support for the involvement of large copy number variants in the pathogenesis of schizophrenia. *Hum Mol Genet* 2009; **18:** 1497-1503.
22. Shaikh TH, Gai X, Perin JC, Glessner JT, Xie H, Murphy K *et al.* High-resolution mapping and analysis of copy number variations in the human genome: a data resource for clinical and research applications. *Genome Res* 2009; **19:** 1682-1690.
23. Altshuler DM, Gibbs RA, Peltonen L, Altshuler DM, Gibbs RA, Peltonen L *et al.* Integrating common and rare genetic variation in diverse human populations. *Nature* 2010; **467:** 52-58.
24. Pinto D, Delaby E, Merico D, Barbosa M, Merikangas A, Klei L *et al.* Convergence of genes and cellular pathways dysregulated in autism spectrum disorders. *Am J Hum Genet* 2014; **94:** 677-694.
25. Sanders SJ, Ercan-Sencicek AG, Hus V, Luo R, Murtha MT, Moreno-De-Luca D *et al.* Multiple recurrent de novo CNVs, including duplications of the 7q11.23 Williams syndrome region, are strongly associated with autism. *Neuron* 2011; **70:** 863-885.
26. Grond-Ginsbach C, Chen B, Pjontek R, Wiest T, Jiang Y, Burwinkel B *et al.* Copy number variation in patients with cervical artery dissection. *Eur J Hum Genet* 2012; **20:** 1295-1299.
27. Silversides CK, Lionel AC, Costain G, Merico D, Migita O, Liu B *et al.* Rare copy number variations in adults with tetralogy of Fallot implicate novel risk gene pathways. *PLoS Genet* 2012; **8:** e1002843.
28. Krepischi AC, Achatz MI, Santos EM, Costa SS, Lisboa BC, Brentani H *et al.* Germline DNA copy number variation in familial and early-onset breast cancer. *Breast Cancer Res* 2012; **14:** R24.
29. Klassen T, Davis C, Goldman A, Burgess D, Chen T, Wheeler D *et al.* Exome sequencing of ion channel genes reveals complex profiles confounding personal risk assessment in epilepsy. *Cell* 2011; **145:** 1036-1048.
30. Purcell SM, Moran JL, Fromer M, Ruderfer D, Solovieff N, Roussos P *et al.* A polygenic burden of rare disruptive mutations in schizophrenia. *Nature* 2014; **506:** 185-190.
31. Piton A, Gauthier J, Hamdan FF, Lafreniere RG, Yang Y, Henrion E *et al.* Systematic resequencing of X-chromosome synaptic genes in autism spectrum disorder and schizophrenia. *Mol Psychiatry* 2011; **16:** 867-880.
32. Chahrour MH, Yu TW, Lim ET, Ataman B, Coulter ME, Hill RS *et al.* Whole-exome sequencing and homozygosity analysis implicate depolarization-regulated neuronal genes in autism. *PLoS Genet* 2012; **8:** e1002635.
33. De Rubeis S, He X, Goldberg AP, Poultney CS, Samocha K, Kou Y *et al.* Synaptic, transcriptional and chromatin genes disrupted in autism. *Nature* 2014; **515:** 209-215.
34. Tarpey PS, Smith R, Pleasance E, Whibley A, Edkins S, Hardy C *et al.* A systematic, large-scale resequencing screen of X-chromosome coding exons in mental retardation. *Nat Genet* 2009; **41:** 535-543.
35. Rauch A, Wieczorek D, Graf E, Wieland T, Endele S, Schwarzmayr T *et al.* Range of genetic mutations associated with severe non-syndromic sporadic intellectual disability: an exome sequencing study. *Lancet* 2012; **380:** 1674-1682.
36. de Ligt J, Willemsen MH, van Bon BW, Kleefstra T, Yntema HG, Kroes T *et al.* Diagnostic exome sequencing in persons with severe intellectual disability. *N Engl J Med* 2012; **367:** 1921-1929.
37. Feng J, Craddock N, Jones IR, Cook EH, Jr., Goldman D, Heston LL *et al.* Systematic screening for mutations in the glycine receptor α2 subunit gene (GLRA2) in patients with schizophrenia and other psychiatric diseases. *Psychiatr Genet* 2001; **11:** 45-48.
38. Iossifov I, Ronemus M, Levy D, Wang Z, Hakker I, Rosenbaum J *et al.* De novo gene disruptions in children on the autistic spectrum. *Neuron* 2012; **74:** 285-299.
39. O'Roak BJ, Vives L, Girirajan S, Karakoc E, Krumm N, Coe BP *et al.* Sporadic autism exomes reveal a highly interconnected protein network of *de novo* mutations. *Nature* 2012; **485:** 246-250.
40. Sanders SJ, Murtha MT, Gupta AR, Murdoch JD, Raubeson MJ, Willsey AJ *et al. De novo* mutations revealed by whole-exome sequencing are strongly associated with autism. *Nature* 2012; **485:** 237-241.
41. Grantham R. Amino acid difference formula to help explain protein evolution. *Science* 1974; **185:** 862-864.
42. Cooper GM, Stone EA, Asimenos G, Green ED, Batzoglou S, Sidow A. Distribution and intensity of constraint in mammalian genomic sequence. *Genome Res* 2005; **15:** 901-913.
43. Ashkenazy H, Erez E, Martz E, Pupko T, Ben-Tal N. ConSurf 2010: calculating evolutionary conservation in sequence and structure of proteins and nucleic acids. *Nucleic Acids Res* 2010; **38:** W529-533.
44. Adzhubei IA, Schmidt S, Peshkin L, Ramensky VE, Gerasimova A, Bork P *et al.* A method and server for predicting damaging missense mutations. *Nat Methods* 2010; **7:** 248-249.
45. Calabrese R, Capriotti E, Fariselli P, Martelli PL, Casadio R. Functional annotations improve the predictive score of human disease-related mutations in proteins. *Hum Mutat* 2009; **30:** 1237-1244.
46. Li B, Krishnan VG, Mort ME, Xin F, Kamati KK, Cooper DN *et al.* Automated inference of molecular mechanisms of disease from amino acid substitutions. *Bioinformatics* 2009; **25:** 2744-2750.
47. Mi H, Muruganujan A, Thomas PD. PANTHER in 2013: modeling the evolution of gene function, and other gene attributes, in the context of phylogenetic trees. *Nucleic Acids Res* 2013; **41:** D377-386.
48. Ng PC, Henikoff S. SIFT: Predicting amino acid changes that affect protein function. *Nucleic Acids Res* 2003; **31:** 3812-3814.